

# OXYGEN REDUCTION ELECTROCATALYSIS

BY

MATTHEW SHERMAN THORUM

DISSERTATION

Submitted in partial fulfillment of the requirements  
for the degree of Doctor of Philosophy in Chemistry  
in the Graduate College of the  
University of Illinois at Urbana-Champaign, 2011

Urbana, Illinois

Doctoral Committee:

Professor Andrew A. Gewirth, Chair  
Professor Paul J. A. Kenis  
Professor Ralph G. Nuzzo  
Professor Thomas B. Rauchfuss

## Abstract

This dissertation is focused on the investigation of the oxygen reduction reaction (ORR) utilizing both existing and newly discovered electrocatalysts. Interest in the ORR is motivated by its application in the cathodes of most fuel cells. The slow kinetics of the ORR are a major barrier to the widespread usage of fuel cells, thus motivating research aimed at increasing understanding of existing electrocatalysts and driving demand for the development of improved electrocatalysts for the ORR.

The first section focuses on laccase, a multicopper oxidase that catalyzes the four-electron reduction of oxygen to water. Upon adsorption to an electrode surface, laccase is known to reduce oxygen at overpotentials lower than the best noble metal electrocatalysts usually employed. Whereas the electrocatalytic activity of laccase is well established on carbon electrodes, laccase does not typically adsorb to better defined noble metal surfaces in an orientation that allows for efficient electrocatalysis. In this work, anthracene-2-methanethiol (AMT) was employed to modify the surface of Au electrodes and the electrocatalytic activity of adsorbed laccase was examined. AMT facilitated the adsorption of laccase, and the onset of electrocatalytic oxygen reduction was observed as high as 1.13  $V_{\text{RHE}}$ . Linear Tafel behavior was observed with a 144 mV/dec slope, consistent with an outer-sphere single-electron transfer from the electrode to a Cu site in the enzyme as the rate-determining step of the oxygen reduction mechanism.

Inspired by the multicopper active site of laccase, the second section focuses on the precipitation of an insoluble complex of copper(II) with 3,5-diamino-1,2,4-triazole onto a carbon black support that leads to the formation of an efficient catalyst for the ORR referred to as CuDAT. The oxygen-reduction activity is reported over a wide pH

range from 1 to 13 and the onset of the ORR occurs at potentials as high as 0.86 V<sub>RHE</sub>, making CuDAT the most active synthetic copper-based electrocatalyst for the ORR reported to date. For the first time, ex situ magnetic susceptibility measurements were used to demonstrate the presence of multicopper sites on the electrode.

The final section addresses the question of whether or not the active sites for the ORR in electrocatalysts based on carbon-supported transition-metal complexes are metal-centered as this has become controversial, especially for heat-treated materials. Some have proposed that the transition metal only serves to form highly active sites based on nitrogen and carbon. Here, we examine the oxygen reduction activity of carbon-supported iron(II) phthalocyanine (FePc) before and after pyrolysis at 800 °C and CuDAT in the presence of several anions and small-molecule poisons, including fluoride, azide, thiocyanate, ethanethiol, and cyanide. CuDAT is poisoned in a manner consistent with a copper-based active site. Although FePc and pyrolyzed FePc are remarkably resilient to most poisons they are poisoned by cyanide indicative of iron-based active sites.

*To Family and Friends*  
*especially Shannon, who is both*

## Acknowledgments

This would not have been possible without the assistance of a large number of people; I cannot name them all here, but I am thankful for their contributions.

Foremost, I need to recognize my advisor, Professor Andrew Gewirth, for providing the resources to make this work possible, for encouraging me to be productive while allowing me to work at my own pace, for teaching me about the research process, for improving written papers, for helpful feedback on oral presentations, for helping sort out career options, and for several baseball metaphors. Next, thanks go to the other members of my doctoral committee, Professors Kenis, Rauchfuss, Masel (who assisted with my preliminary exam), and Nuzzo (who assisted with my final defense) for their time, insights, and constructive feedback. Fruitful collaborations with Professors Zimmerman, Lu, and Kenis and their students (especially Cyrus Anderson, Nick Marshall, Bryant Kearn, and Fik Brushett) made several publications possible.

Members of the Gewirth Group made enduring the up's and down's of research fun (or at least tolerable, depending on the week). Former members Tighe Spurlin, Karen Stewart, Scott Shaw, Ezra Eibergen, and Clinton King helped me get my feet on the ground and figure out where stuff was. Andrew Campbell and Jeremy Hatch were here for the whole ride and provided motivation, friendly competition, lengthy discussions, and lots of laughs. Thanks also go to current group members Matt Thorseth, Dennis Butcher, Brandon Long, Nicole Honesty, Joe Buthker, Claire Tornow, Laura Huff, Tom Mahle, Adele Pacquette, Justin Oberst, and Hadi Tavassol for continuing to provide an interesting research environment.

Outside of the lab, the UIUC Climbing Club provided a new hobby and friends; climbing partners James Fran, Rich Weston, Doug Johnson, Tzlil Perahia, and Tom Butler helped me escape and renew my excitement to be here. Fellow members of the University Ward of the Church of Jesus Christ of Latter-day Saints provided a diverse and supportive community that encouraged me to grow and improve.

My brothers, parents, grandparents and other family provided the inspiration to start and the motivation to push on to the end. Finally, my wife Shannon has simply made things better; I will always appreciate her love, patience, and productivity (and hope that more of these will rub off).

## Table of Contents

<b>CHAPTER 1. Introduction.....</b>	<b>1</b>
<b>CHAPTER 2. Experimental Procedures .....</b>	<b>16</b>
<b>CHAPTER 3. Direct, Electrocatalytic Oxygen Reduction by Laccase on Anthracene-2-methanethiol-Modified Gold .....</b>	<b>25</b>
<b>CHAPTER 4. Oxygen Reduction Activity of a Copper Complex with 3,5-Diamino-1,2,4-triazole Supported on Carbon Black.....</b>	<b>42</b>
<b>CHAPTER 5. Poisoning the Oxygen Reduction Reaction on Carbon- Supported Fe and Cu Electrocatalysts: Evidence for Metal-Centered Activity .....</b>	<b>57</b>
<b>Appendix A. Gold Roughening Macro .....</b>	<b>70</b>
<b>Author's Curriculum Vitae .....</b>	<b>71</b>

## CHAPTER 1. Introduction

### Background

#### *The Oxygen Reduction Reaction*

Although the oxygen reduction reaction (ORR) is important in variety of electrochemical processes and technologies including corrosion (and corrosion inhibition), sensors, and metal-air batteries, the application of the ORR in fuel cells is of particular interest.<sup>1-4</sup> A fuel cell is an electrochemical device, similar to a battery, that generates an electrical potential through the oxidation of a fuel at an anode electrode and the reduction of an oxidant at a cathode electrode. The anode and cathode are separated by an electrolyte that permits the mass-transfer of ions between the electrodes. In contrast to batteries that must be recharged electrically or discarded when their reactants are consumed, reactants are replenished or continuously supplied in a fuel cell. While a variety of fuels may be used as electron sources at the anode (including hydrogen, methanol, and formic acid etc.) the ubiquity of oxygen in the atmosphere and the large thermodynamic driving force of the oxygen reduction reaction make oxygen the most appealing oxidant for most fuel cell cathodes.<sup>3</sup> The desired reaction is the four electron reduction of oxygen to water (Equation 1.1), the two electron reduction of oxygen to hydrogen peroxide (Equation 1.2) is less desirable because of the lower efficiency and the generation of corrosive peroxide associated with it.<sup>3</sup>



Although the 1.23 V reduction potential of the ORR provides a substantial thermodynamic driving force the reaction is kinetically slow. The sluggish kinetics of the



ORR are typically attributed to the strength of the O=O bond (498 kJ/mol) that must be broken in the course of the reaction.<sup>1</sup> In order to obtain meaningful current densities from the electroreduction of oxygen the kinetics of the ORR must be increased by lowering the activation energy of the reaction. The activation energy is lowered through the use of electrocatalysts and also by reducing the electrode potential. The difference between the electrode potential ( $E$ ) and the equilibrium potential ( $E_{\text{eq}}$ , 1.23 V for the ORR) of the electrode reaction is known as the overpotential,  $\eta$  (Equation 1.3).<sup>5</sup>

$$\eta = E - E_{\text{eq}} \quad (1.3)$$

When the current of an electrochemical reaction is limited solely by the kinetics of the electrode reaction at large overpotentials ( $\eta > 0.12$  V), the relationship between the current ( $i$ ) and the overpotential ( $\eta$ ) is described by the Tafel equation (Equation 1.4 or 1.5)

$$i = i_0 e^{-\frac{\alpha\eta F}{RT}} \quad (1.4)$$

or

$$\eta = \frac{RT}{\alpha F} \ln i_0 - \frac{RT}{\alpha F} \ln i \quad (1.5)$$

where  $i_0$  is the exchange current,  $\alpha$  is the transfer coefficient, and  $T$  is temperature;  $R$  and  $F$  are constants with their typical meanings.<sup>5-6</sup> At the equilibrium potential ( $E_{\text{eq}}$ ) a dynamic equilibrium exists where the rate of the forward reaction is equal to the rate of the reverse reaction, the exchange current ( $i_0$ ) describes the rate of these forward and reverse reactions which are equal in magnitude and sum to zero net flow of current. Increasing the overpotential lowers the activation barrier of the reaction in a linear fashion and, at sufficient overpotentials, the current increases exponentially as a function of the overpotential. The transfer coefficient ( $\alpha$ ) is the proportionality coefficient between

the overpotential and the activation barrier. At large overpotentials the current eventually becomes limited by Ohmic losses and by the mass-transport of oxygen to the electrode surface.

Electrocatalysts act to increase the exchange current and therefore the increase current at all overpotentials where the observed current is kinetically limited (Equation 1.4). Although a comparison of the exchange currents of the ORR would be the most precise way to compare electrocatalysts, this comparison is impractical because with most electrocatalysts the exchange current of the ORR is several orders of magnitude smaller than the observed currents. Although a value for the exchange current may be calculated by extrapolation from a plot of  $\log i$  versus  $\eta$  using the Tafel equation (1.5), a so called Tafel plot, this extrapolation introduces large uncertainties.<sup>2,5</sup> In practice, electrocatalysts are compared in one of two ways: (1) Two similar electrocatalysts are best compared by comparing the observed current densities of the ORR at a given potential, but this comparison is only possible if the current is under kinetic control with both electrocatalysts at the desired potential.<sup>2</sup> (2) If the activities of the electrocatalysts differ by an amount that precludes evaluation at the same potential, then it is preferable to compare their onset potentials ( $E_{\text{onset}}$ ), where the onset potential is the potential at which a given (small) current density is reached, and that current density is chosen to roughly correspond the lowest value readily distinguished from zero by eye.<sup>7</sup> The comparison of onset potentials is somewhat arbitrary and imprecise, but it is very useful for qualitatively ranking electrocatalysts over a wide range of activities

The most widely used electrocatalysts for the ORR are based on platinum and its alloys. However, even with these platinum catalysts, the onset of the ORR occurs at a

large overpotential of about 300 mV (corresponding to an electrode potential of about 0.9 V), still larger overpotentials of 500–600 mV are required to obtain useful current densities.<sup>1</sup> Due to the scarcity and high cost of platinum, a large research effort has focused on reducing the platinum loading in fuel cell cathodes, and these efforts have been fairly successful at meeting the DOE targets required for the widespread usage of fuel cells.<sup>8</sup> However, reducing the platinum loading does not reduce the overpotential associated with the oxygen reduction reaction. Even with the best platinum catalysts, the overpotentials required to overcome the slow kinetics of the ORR result in dramatic losses in efficiency (over 25%).<sup>2-3</sup> The development of electrocatalysts with a higher activity than platinum would lead to large increases in fuel cell efficiency and large reductions in fuel cell costs greatly facilitating the transition of fuel cells into practical usage.

#### *Oxygen Reduction Activity of Laccase<sup>1</sup>*

Although platinum-based electrocatalysts are the most widely used in practical applications, the highest activity ORR catalysts are actually found in implementations using laccase, a type of multicopper oxidase enzyme.<sup>9</sup> Laccase couples the oxidation of substrate to the four-electron reduction of oxygen. The ORR onset potential for laccase-modified electrodes can approach the 1.2 V reversible potential of the ORR; at 0.9 V, where platinum activity is typically evaluated, the current is limited by the rate of diffusion of oxygen to the electrode surface rather than the kinetics of the ORR.<sup>10</sup> The oxygen molecule is activated at a tricopper site and the substrate is oxidized remotely at a separate monocopper site.<sup>11</sup> The ORR mechanism of laccase is described in detail in Chapter 3. The spatial separation between oxygen activation and substrate oxidation

makes laccase amenable to application as an electrocatalyst upon establishing electron transfer with an electrode surface in lieu of substrate oxidation.<sup>12</sup>

Two general strategies have been employed to attach laccase to electrode surfaces and establish electronic communication. The first utilizes an electron-transfer mediator, typically an osmium complex, to shuttle electrons between the enzyme and the electrode surface.<sup>10, 13-20</sup> This method allows thick layers of enzyme to be used, leading to good durability and larger current densities. The potential of the electrode is however determined by the mediator. Direct electron transfer between laccase and carbon electrodes can also be established by utilizing a diazonium coupling reaction to modify the electrode surface with polycyclic aromatic molecules (such as anthracene).<sup>12, 21</sup> These aromatic linkers facilitate binding of laccase to the electrode, apparently in a favorable orientation, and assist in electron transfer to the active site. Direct electron transfer eliminates the need for a mediator so the electrode activity is determined by the enzyme. Such thin films of enzyme are however less durable and support lower current densities than mediated electrodes.<sup>11</sup> In spite of their activity at remarkably high potential, significant barriers preclude the practical use of enzyme-modified electrodes including high cost, limited durability, limited pH ranges (4–7), and low power densities due to low surface coverage.<sup>22-23</sup>

Even though it is unlikely that laccase can be used as a practical electrocatalyst for the ORR in a typical fuel cell, its remarkable ORR activity proves that it is possible to develop electrocatalysts with greater activities than platinum and that it is possible to do so using nonprecious metals (copper in the case of laccase).

### *Nonprecious Metal (NPM) Electrocatalysts for the ORR*

The high cost and scarcity of Pt has motivated longstanding research interests into nonprecious metal (NPM) electrocatalysts for the ORR.<sup>1-3, 24-25</sup> One of the most interesting and versatile approaches towards the development of NPM electrocatalysts has been in the area of transition-metal coordination complexes. Early work was initiated in 1964 by Jasinski's discovery that the ORR activity of nickel electrodes was increased by coating them with cobalt phthalocyanine.<sup>26</sup> A large amount of research activity into the use of dyestuffs for the ORR followed largely focusing on transition metal porphyrins and phthalocyanines (Figure 1.1).<sup>27-29</sup> It was found that complexes of iron and cobalt tended to have the highest activities, although the activities were generally lower than Pt and suffered from a lack of stability. Collman and Anson's work in the 1980's found improvements in activity through the use of bis-cofacial cobalt porphyrins (Figure 1.1).<sup>30-32</sup> More recently, other means of tailoring the metal-metal distance between the macrocycles have employed "pac-man" porphyrins that link the macrocycles together with a flexible tether.<sup>33-34</sup> Work on transition-metal macrocycles continues today, although substantial increases in activity are elusive.<sup>35</sup>

There are few reports of synthetic copper complexes that exhibit significant ORR activity.<sup>7</sup> Several mononuclear Cu complexes have been investigated via adsorption onto graphite electrodes.<sup>36-41</sup> Copper(II) complexes with phenanthroline ligands, which were popularized by Zhang and Anson,<sup>38</sup> are the best-studied to date (Figure 1.1). McCrory et al. have investigated the copper complexes of a variety of substituted phenanthrolines, the best of which demonstrated an ORR onset of about 0.68 V at pH 4.8, and concluded that further increases in activity were unlikely with this system.<sup>39</sup> Attempts that used putative multicopper complexes include a water soluble catalyst formed by the coordination of

two copper(II) ions in a hexaazamacrocyclic ligand,<sup>42</sup> and electrodes modified with solution-cast polymers containing copper(II) ions, including a copper–poly(histidine) complex,<sup>43</sup> and a polymeric copper(II) oxalato complex.<sup>44</sup> The demonstration of polynuclearity when adsorbed on an electrode in any of these systems is lacking. A cytochrome *c* oxidase model compound with a Cu–Fe site has also been investigated by adsorption onto graphite, but the ORR onset is quite low at about 0.2 V and the complex that contains only Fe has similar activity.<sup>45</sup>

A major issue that haunts all work on the ORR activity of transition-metal coordination complexes is uncertainty regarding the nature of the active site after the complex is adsorbed onto the electrode surface. In the early 1970's it was discovered that the activity and the durability of electrodes modified with iron or cobalt macrocycles can be improved by heat-treating them under an inert atmosphere.<sup>27-29</sup> The use of high temperatures (600–900 °C) led to the best materials and also resulted in the complete decomposition of the macrocycle.<sup>46-48</sup> Furthermore, other simple iron and nitrogen sources (such as iron acetate and ammonia) can be used in place of the metal macrocycle.<sup>48-51</sup> Yeager proposed that decomposition of the macrocycle at high temperatures forms a nitrogen-rich surface on a carbon electrode that is capable of coordinating iron (or other transition metals) to form ORR active sites.<sup>47</sup> Yeager's work showed that the macrocycles remain intact on the carbon surface prior to heat treatment,<sup>46</sup> although the similarity in the ORR activity before and after heat treatment leads to some doubt about whether the intact macrocycles are in fact ORR active.<sup>1</sup> The ORR activity of these heat-treated Fe/N/C materials can rival that of platinum, although durability continues to preclude practical usage.<sup>51</sup>

More recently it has been shown that “metal free” materials based on carbon and nitrogen exhibit substantial ORR activity, especially in base.<sup>52-57</sup> It has also been found that carbon monoxide does not poison heat-treated Fe/N/C electrocatalysts.<sup>58</sup> These observations lead to doubt that any of these materials feature metallic active sites. The higher activity that results from metal-containing precursors is attributed to the metals acting as catalysts to form N/C in a highly active morphology.<sup>54</sup> Others maintain that the “metal free” materials contain trace amounts of iron and that carbon monoxide is merely a poor choice of poison.<sup>47, 59</sup>

In spite of these challenges (and partially because of them) work on transitional metal complexes as electrocatalysts for the ORR remains an active area of research. The tremendous appeal of a low-cost (and potentially higher activity) alternative to platinum electrocatalysts in fuel cell cathodes will continue to drive interest in this area.

## **Research Goals**

The research described in this dissertation seeks to improve understanding about the mechanism and reactivity of several oxygen reduction electrocatalysts and apply that understanding towards the development of new electrocatalysts for the oxygen reduction reaction.

In chapter 3, the oxygen reduction activity of laccase from *Trametes versicolor* (*TvLc*) is evaluated on a thiol-modified gold electrode. Although anthracene-modified carbon has yielded success in obtaining direct electrocatalytic reduction of oxygen by laccase on carbon electrodes, direct electrocatalysis on gold has not been previously reported for *TvLc*. Characterization of *TvLc* on a better defined noble metal surface, such as gold, is desired to provide a potentially superior analytical platform. A strategy for obtaining direct electron transfer between the enzyme and a gold surface is outlined, and

successfully implemented. Insights into the oxygen reduction mechanism of the *TvLc* modified gold electrode are also described.

In chapter 4, the discovery of a new copper-based electrocatalyst (CuDAT), inspired by the active site of laccase, is described. For the first time, multicopper sites are observed on the electrode surface through the use of magnetic susceptibility measurements. The oxygen reduction activity is characterized using rotating ring-disk electrode voltammetry and found to be the highest known for any synthetic copper-based material.

In chapter 5, a systematic study of the effects of several poisons on the oxygen reduction activity of several NPM electrocatalysts for the ORR is described. Evidence for metal-centered activity in Fe/N/C and CuDAT is presented and evaluated. The failure of prior poisoning studies is also explained.



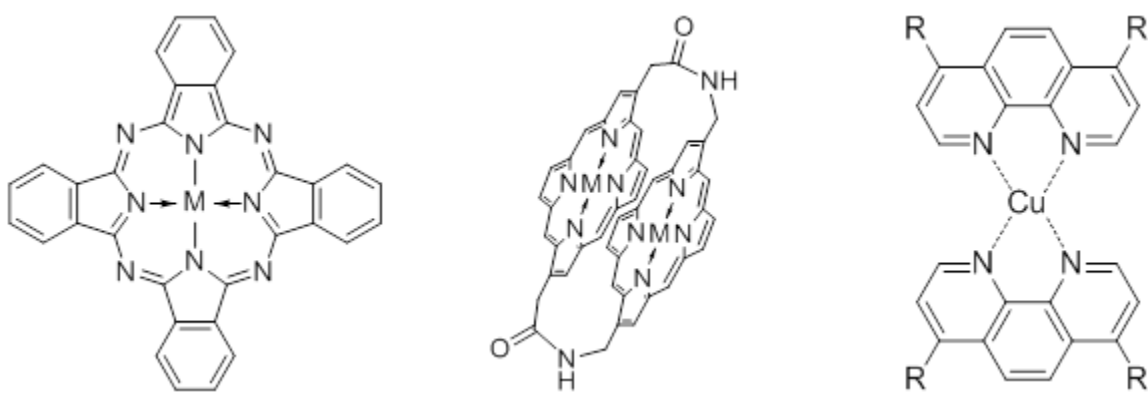


**Figure 1.1.** Examples of typical transition-metal complexes that have been used as electrocatalysts for the ORR including metal phthalocyanines (left), bis-cofacial porphyrins (center), and copper phenanthrolines (right).

## References

- (1) Gewirth, A. A.; Thorum, M. S., Electroreduction of Dioxygen for Fuel-Cell Applications: Materials and Challenges. *Inorg. Chem.* **2010**, *49*, 3557-3566.
- (2) Gasteiger, H. A.; Kocha, S. S.; Sompalli, B.; Wagner, F. T., Activity Benchmarks and Requirements for Pt, Pt-Alloy, and Non-Pt Oxygen Reduction Catalysts for PEMFCs. *Appl. Catal., B* **2005**, *56*, 9-35.
- (3) Vielstich, W.; Lamm, A.; Gasteiger, H. A.; Yokokawa, H., *Handbook of Fuel Cells :Fundamentals, Technology and Applications*. Wiley: Chichester, England, 2003.
- (4) Wagner, F. T.; Lakshmanan, B.; Mathias, M. F., Electrochemistry and the Future of the Automobile. *J. Phys. Chem. Lett.* **2010**, *1*, 2204-2219.
- (5) Bard, A. J.; Faulkner, L. R., *Electrochemical Methods: Fundamentals and Applications*. Wiley: New York, 2001.
- (6) Bockris, J. O. M.; Reddy, A. K., *Modern Electrochemistry*. Plenum Press: New York, 1973; Vol. 2.
- (7) Thorum, M. S.; Yadav, J.; Gewirth, A. A., Oxygen Reduction Activity of a Copper Complex of 3,5-Diamino-1,2,4-Triazole Supported on Carbon Black. *Angew. Chem., Int. Ed.* **2009**, *48*, 165-167.
- (8) Spendelow, J.; Epping Martin, K.; Papageorgopoulos, D., DOE Hydrogen Program Record #9018. 2010  
[http://www.hydrogen.energy.gov/pdfs/9018\\_platinum\\_group.pdf](http://www.hydrogen.energy.gov/pdfs/9018_platinum_group.pdf)
- (9) Solomon, E. I.; Sundaram, U. M.; Machonkin, T. E., Multicopper Oxidases and Oxygenases. *Chem. Rev.* **1996**, *96*, 2563-2605.
- (10) Mano, N.; Soukharev, V.; Heller, A., A Laccase-Wiring Redox Hydrogel for Efficient Catalysis of O<sub>2</sub> Electroreduction. *J. Phys. Chem. B* **2006**, *110*, 11180-11187.
- (11) Cracknell, J. A.; Vincent, K. A.; Armstrong, F. A., Enzymes as Working or Inspirational Electrocatalysts for Fuel Cells and Electrolysis. *Chem. Rev.* **2008**, *108*, 2439-2461.
- (12) Blanford, C. F.; Foster, C. E.; Heath, R. S.; Armstrong, F. A., Efficient Electrocatalytic Oxygen Reduction by the 'Blue' Copper Oxidase, Laccase, Directly Attached to Chemically Modified Carbons. *Faraday Discuss.* **2009**, *140*, 319-335.
- (13) Gallaway, J. W.; Calabrese Barton, S. A., Kinetics of Redox Polymer-Mediated Enzyme Electrodes. *J. Am. Chem. Soc.* **2008**, *130*, 8527-8536.

- (14) Hudak, N. S.; Gallaway, J. W.; Barton, S. C., Mediated Biocatalytic Cathodes Operating on Gas-Phase Air and Oxygen in Fuel Cells. *J. Electrochem. Soc.* **2009**, *156*, B9-B15.
- (15) Hudak, N. S.; Gallaway, J. W.; Barton, S. C., Formation of Mediated Biocatalytic Cathodes by Electrodeposition of a Redox Polymer and Laccase. *J. Electroanal. Chem.* **2009**, *629*, 57-62.
- (16) Gallaway, J.; Wheeldon, I.; Rincon, R.; Atanassov, P.; Banta, S.; Barton, S. C., Oxygen-Reducing Enzyme Cathodes Produced from SLAC, a Small Laccase from *Streptomyces coelicolor*. *Biosens. Bioelectron.* **2008**, *23*, 1229-1235.
- (17) Soukharev, V.; Mano, N.; Heller, A., A Four-Electron O<sub>2</sub>-Electroreduction Biocatalyst Superior to Platinum and a Biofuel Cell Operating at 0.88 V. *J. Am. Chem. Soc.* **2004**, *126*, 8368-8369.
- (18) Barton, S. C.; Pickard, M.; Vazquez-Duhalt, R.; Heller, A., Electroreduction of O<sub>2</sub> to Water at 0.6 V (SHE) at pH 7 on the 'Wired' *Pleurotus ostreatus* Laccase Cathode. *Biosens. Bioelectron.* **2002**, *17*, 1071-1074.
- (19) Barton, S. C.; Kim, H. H.; Binyamin, G.; Zhang, Y. C.; Heller, A., The "Wired" Laccase Cathode: High Current Density Electroreduction of O<sub>2</sub> to Water at +0.7 V (NHE) at pH 5. *J. Am. Chem. Soc.* **2001**, *123*, 5802-5803.
- (20) Barton, S. C.; Kim, H. H.; Binyamin, G.; Zhang, Y. C.; Heller, A., Electroreduction of O<sub>2</sub> to Water on the "Wired" Laccase Cathode. *J. Phys. Chem. B* **2001**, *105*, 11917-11921.
- (21) Blanford, C. F.; Heath, R. S.; Armstrong, F. A., A Stable Electrode for High-Potential, Electrocatalytic O<sub>2</sub> Reduction Based on Rational Attachment of a Blue Copper Oxidase to a Graphite Surface. *Chem. Commun.* **2007**, 1710-1712.
- (22) Barton, S. C.; Gallaway, J.; Atanassov, P., Enzymatic Biofuel Cells for Implantable and Microscale Devices. *Chem. Rev.* **2004**, *104*, 4867-4886.
- (23) General Discussion. *Faraday Discuss.* **2009**, *140*, 417-437.
- (24) Gasteiger, H. A.; Markovic, N. M., Just a Dream-or Future Reality? *Science* **2009**, *324*, 48-49.
- (25) Jaouen, F.; Proietti, E.; Lefevre, M.; Chenitz, R.; Dodelet, J. P.; Wu, G.; Chung, H. T.; Johnston, C. M.; Zelenay, P., Recent Advances in Non-Precious Metal Catalysis for Oxygen-Reduction Reaction in Polymer Electrolyte Fuel Cells. *Energy & Environmental Science* **2011**, *4*, 114-130.
- (26) Jasinski, R., New Fuel Cell Cathode Catalyst. *Nature* **1964**, *201*, 1212.

- (27) Alt, H.; Binder, H.; Sandstede, G., Mechanism of the Electrocatalytic Reduction of Oxygen on Metal Chelates. *J. Catal.* **1973**, *28*, 8-19.
- (28) Jahnke, H.; Schönborn, M.; Zimmermann, G., Organic Dyestuffs as Catalysts for Fuel Cells. In *Physical and Chemical Applications of Dyestuffs*, Schäfer, F.; Gerischer, H.; Willig, F.; Meier, H.; Jahnke, H.; Schönborn, M.; Zimmermann, G., Eds. Springer Berlin / Heidelberg: 1976; Vol. 61, pp 133-181.
- (29) Bagotzky, V. S.; Tarasevich, M. R.; Radyushkina, K. A.; Levina, O. A.; Andrusyova, S. I., Electrocatalysis of the Oxygen Reduction Process on Metal Chelates in Acid Electrolyte. *J. Power Sources* **1977**, *2*, 233-240.
- (30) Collman, J. P.; Denisevich, P.; Konai, Y.; Marrocco, M.; Koval, C.; Anson, F. C., Electrode Catalysis of the Four-Electron Reduction of Oxygen to Water by Dicobalt Face-to-Face Porphyrins. *J. Am. Chem. Soc.* **1980**, *102*, 6027-6036.
- (31) Collman, J. P.; Bencosme, C. S.; Durand, R. R.; Kreh, R. P.; Anson, F. C., Mixed-Metal Face-to-Face Porphyrin Dimers. *J. Am. Chem. Soc.* **1983**, *105*, 2699-2703.
- (32) Durand, R. R.; Bencosme, C. S.; Collman, J. P.; Anson, F. C., Mechanistic Aspects of the Catalytic Reduction of Dioxygen by Cofacial Metalloporphyrins. *J. Am. Chem. Soc.* **1983**, *105*, 2710-2718.
- (33) Chang, C. J.; Deng, Y.; Shi, C.; Chang, C. K.; Anson, F. C.; Nocera, D. G., Electrocatalytic Four-Electron Reduction of Oxygen to Water by a Highly Flexible Cofacial Cobalt Bisporphyrin. *Chem. Commun.* **2000**, 1355-1356.
- (34) Chang, C. J.; Loh, Z. H.; Shi, C.; Anson, F. C.; Nocera, D. G., Targeted Proton Delivery in the Catalyzed Reduction of Oxygen to Water by Bimetallic Pacman Porphyrins. *J. Am. Chem. Soc.* **2004**, *126*, 10013-10020.
- (35) Li, W.; Yu, A.; Higgins, D. C.; Llanos, B. G.; Chen, Z., Biologically Inspired Highly Durable Iron Phthalocyanine Catalysts for Oxygen Reduction Reaction in Polymer Electrolyte Membrane Fuel Cells. *J. Am. Chem. Soc.* **2010**, *132*, 17056-17058.
- (36) Zhang, J.; Anson, F. C., Complexes of Cu(II) with Electroactive Chelating Ligands Adsorbed on Graphite Electrodes: Surface Coordination Chemistry and Electrocatalysis. *J. Electroanal. Chem.* **1993**, *348*, 81-97.
- (37) Dias, V. L. N.; Fernandes, E. N.; da Silva, L. M. S.; Marques, E. P.; Zhang, J.; Marques, A. L. B., Electrochemical Reduction of Oxygen and Hydrogen Peroxide Catalyzed by a Surface Copper(II)-2,4,6-Tris(2-Piridil)-1,3,5-Triazine Complex Adsorbed on a Graphite Electrode. *J. Power Sources* **2005**, *142*, 10-17.

- (38) Zhang, J.; Anson, F. C., Electrochemistry of the Cu(II) Complex of 4,7-Diphenyl-1,10-Phenanthrolinedisulfonate Adsorbed on Graphite Electrodes and Its Behavior as an Electrocatalyst for the Reduction of O<sub>2</sub> and H<sub>2</sub>O<sub>2</sub>. *J. Electroanal. Chem.* **1992**, *341*, 323-341.
- (39) McCrory, C. C. L.; Ottenwaelder, X.; Stack, T. D. P.; Chidsey, C. E. D., Kinetic and Mechanistic Studies of the Electrocatalytic Reduction of O<sub>2</sub> to H<sub>2</sub>O with Mononuclear Cu Complexes of Substituted 1,10-Phenanthrolines. *J. Phys. Chem. A* **2007**, *111*, 12641-12650.
- (40) Cai, C. X.; Xue, K. H.; Xu, X. Y.; Luo, Q. H., Electrocatalysis for the Reduction of O<sub>2</sub> and H<sub>2</sub>O<sub>2</sub> Based on Complex of Copper(II) with the Tris(3-Aminopropyl)Amine and Imidazole Ligands. *J. Appl. Electrochem.* **1997**, *27*, 793-798.
- (41) Wang, M.; Xu, X.; Gao, J.; Jia, N.; Cheng, Y., Electrocatalytic Reduction of O<sub>2</sub> at Pyrolytic Graphite Electrode Modified by a Novel Copper(II) Complex with 2-[Bis(2-Aminoethyl)Amino]Ethanol and Imidazole Ligands. *Russ. J. Electrochem.* **2006**, *42*, 878-881.
- (42) Slowinski, K.; Kublik, Z.; Bilewicz, R.; Pietraszkiewicz, M., Electrocatalysis of Oxygen Reduction by a Copper(II) Hexaazamacrocyclic Complex. *Chem. Commun.* **1994**, 1087-1088.
- (43) Weng, Y. C.; Fan, F. R. F.; Bard, A. J., Combinatorial Biomimetics. Optimization of a Composition of Copper(II) Poly-L-Histidine Complex as an Electrocatalyst for O<sub>2</sub> Reduction by Scanning Electrochemical Microscopy. *J. Am. Chem. Soc.* **2005**, *127*, 17576-17577.
- (44) Kim, J.; Gewirth, A. A., Electrocatalysis of Oxygen Reduction by Cu-Containing Polymer Films on Glassy Carbon Electrodes. *Bull. Korean Chem. Soc.* **2007**, *28*, 1322-1328.
- (45) Shin, H.; Lee, D.-H.; Kang, C.; Karlin, K. D., Electrocatalytic Four-Electron Reductions of O<sub>2</sub> to H<sub>2</sub>O with Cytochrome C Oxidase Model Compounds. *Electrochim. Acta* **2003**, *48*, 4077-4082.
- (46) Scherson, D. A.; Yao, S. B.; Yeager, E. B.; Eldridge, J.; Kordesch, M. E.; Hoffman, R. W., In Situ and Ex Situ Moessbauer Spectroscopy Studies of Iron Phthalocyanine Adsorbed on High Surface Area Carbon. *J. Phys. Chem.* **1983**, *87*, 932-943.
- (47) Yeager, E., Electrocatalysts for O<sub>2</sub> Reduction. *Electrochim. Acta* **1984**, *29*, 1527-1537.
- (48) Gupta, S.; Tryk, D.; Bae, I.; Aldred, W.; Yeager, E., Heat-Treated Polyacrylonitrile-Based Catalysts for Oxygen Electroreduction. *J. Appl. Electrochem.* **1989**, *19*, 19-27.

- (49) Faubert, G.; Côté, R.; Dodelet, J. P.; Lefèvre, M.; Bertrand, P., Oxygen Reduction Catalysts for Polymer Electrolyte Fuel Cells from the Pyrolysis of Fe<sup>II</sup> Acetate Adsorbed on 3,4,9,10-Perylenetetracarboxylic Dianhydride. *Electrochim. Acta* **1999**, *44*, 2589-2603.
- (50) Jaouen, F.; Marcotte, S.; Dodelet, J. P.; Lindbergh, G., Oxygen Reduction Catalysts for Polymer Electrolyte Fuel Cells from the Pyrolysis of Iron Acetate Adsorbed on Various Carbon Supports. *J. Phys. Chem. B* **2003**, *107*, 1376-1386.
- (51) Lefevre, M.; Proietti, E.; Jaouen, F.; Dodelet, J. P., Iron-Based Catalysts with Improved Oxygen Reduction Activity in Polymer Electrolyte Fuel Cells. *Science* **2009**, *324*, 71-74.
- (52) Maldonado, S.; Stevenson, K. J., Direct Preparation of Carbon Nanofiber Electrodes Via Pyrolysis of Iron(II) Phthalocyanine: Electrocatalytic Aspects for Oxygen Reduction. *J. Phys. Chem. B* **2004**, *108*, 11375-11383.
- (53) Matter, P. H.; Wang, E.; Arias, M.; Biddinger, E. J.; Ozkan, U. S., Oxygen Reduction Reaction Activity and Surface Properties of Nanostructured Nitrogen-Containing Carbon. *J. Mol. Catal. A: Chem.* **2007**, *264*, 73-81.
- (54) Biddinger, E.; von Deak, D.; Ozkan, U., Nitrogen-Containing Carbon Nanostructures as Oxygen-Reduction Catalysts. *Top. Catal.* **2009**, *52*, 1566-1574.
- (55) Biddinger, E. J.; Ozkan, U. S., Role of Graphitic Edge Plane Exposure in Carbon Nanostructures for Oxygen Reduction Reaction. *J. Phys. Chem. C* **2010**, *114*, 15306-15314.
- (56) Gong, K.; Du, F.; Xia, Z.; Durstock, M.; Dai, L., Nitrogen-Doped Carbon Nanotube Arrays with High Electrocatalytic Activity for Oxygen Reduction. *Science* **2009**, *323*, 760-764.
- (57) Yu, D.; Nagelli, E.; Du, F.; Dai, L., Metal-Free Carbon Nanomaterials Become More Active Than Metal Catalysts and Last Longer. *J. Phys. Chem. Lett.* **2010**, *1*, 2165-2173.
- (58) Maldonado, S.; Stevenson, K. J., Influence of Nitrogen Doping on Oxygen Reduction Electrocatalysis at Carbon Nanofiber Electrodes. *J. Phys. Chem. B* **2005**, *109*, 4707-4716.
- (59) Birry, L.; Zagal, J. H.; Dodelet, J.-P., Does CO Poison Fe-Based Catalysts for ORR? *Electrochem. Commun.* **2010**, *12*, 628-631.

## CHAPTER 2. Experimental Procedures

### General Procedures

#### *Cleaning*

In order to ensure accuracy and reproducibility in electrochemical experiments careful attention to must be paid to the cleanliness and usage history of the equipment used this is especially important for any glassware or other equipment that comes into direct contact with electrolyte solutions. Glassware used to prepare or store electrolyte solutions and glass electrochemical cells were cleaned with the following procedure. This procedure is also suitable for cleaning components made from Teflon<sup>®</sup> or other fluorinated polymers, quartz, and some types of poly(ethylene) or poly(propylene). First, all residues from prior experiments are removed using standard procedures (*e.g.* washing with soap and water or a suitable solvent) and the equipment is rinsed with deionized (DI) water. After rinsing, the equipment is transferred to a bath containing concentrated sulfuric acid and NoChromix<sup>®</sup> (Godax Laboratories) where it is allowed to soak for several hours or overnight to oxidize and remove any organic contaminants. The sulfuric acid residue is rinsed away with DI water and the equipment is placed in a bath containing 35% nitric acid for several hours to remove any metallic contaminants or remaining sulfuric acid residues. The nitric acid is removed by rinsing with DI water. Finally, all equipment is rinsed with boiling purified water (Milli-Q Reference, 18.2 M $\Omega$ ). This final rinse with boiling water should be performed immediately before use of the clean equipment. Simply rinsing glassware with boiling Milli-Q water was found to be sufficient if no contamination occurs during usage and the composition of the electrolyte does not change between experiments.

### *Electrolyte Preparation*

All electrolytes were prepared using purified water (Milli-Q Reference, 18.2 M $\Omega$ ), clean glassware (see above), and commercial reagents of the highest available purity without further purification. Electrolyte solutions were stored, tightly closed, in either clean glassware or FEP containers with the exception of NaOH solutions which were stored in HDPE (to avoid silicate contamination). The electrolyte for the evaluation of laccase-modified electrodes was citrate-phosphate buffer prepared by adjusting the pH of citric acid (0.1M) to 4.00 with Na<sub>2</sub>HPO<sub>4</sub> (0.2 M). Britton-Robinson<sup>1</sup> buffers were used to compare the activity of an electrode across a range of pH values without changing the counter-ions present in solution and were prepared to contain: NaClO<sub>4</sub> (0.1 M), acetic acid (0.04 M), phosphoric acid (0.04 M), and boric acid (0.04 M); the pH was adjusted to the desired value with NaOH (0.1 M). Routine experiments were also conducted in a commercially available pH 6.0 phosphate buffer solution (0.05 M, Fisher Scientific) without issues.

### **Gold Working Electrode Preparation**

#### *Polished Polycrystalline Gold*

Polycrystalline gold disks were 10 mm in diameter (Monocrystals Co.) and were mechanically polished by hand using successively finer diamond suspensions (9  $\mu$ m, 3  $\mu$ m, 1  $\mu$ m, 0.3  $\mu$ m, and 0.05  $\mu$ m, Buehler) on MicroCloth<sup>®</sup> disks (Buehler) adhered to a flat glass plate. After each polishing step the electrodes were rinsed and sonicated in ultrapure water. Polished electrodes were stored under ultrapure water when not in use. Polished electrodes were flame annealed in a hydrogen flame until red hot for 10 min and then allowed to cool in air for 8 min before use.<sup>2</sup>



### *Electrochemically Roughened Gold*

Polycrystalline gold disks were 10 mm in diameter (Monocrystals Co.) and were mechanically polished on an EcoMet 3000 variable speed polisher (Buehler) using a slurry containing 9.5  $\mu\text{m}$  alumina powder (Buehler) on a MicroCloth<sup>®</sup> disk (Buehler). After polishing, residual alumina is removed by rinsing and sonicating in ultrapure water and the electrode surface is wiped dry with a Kimwipe<sup>®</sup> (wiping was found to improve the roughening consistency). Electrochemical roughening is performed using a KCl (0.5 M) electrolyte, a gold counter electrode prepared from gold wire to have a surface area greater than the working electrode, and a Ag/AgCl reference electrode (BAS) in a beaker open to the air. Roughening is accomplished by applying a series of oxidation and reduction cycles that are based on published procedures.<sup>3-4</sup> A diagram of the potential waveform and a macro program written for a CH Instruments potentiostat are included as Appendix A. After roughening, the gold electrode has a uniform dark red-brown color and is rinsed with ultrapure water and kept under water.

### *Thiol Modification*

Anthracene-2-methanethiol (AMT) was synthesized by Cyrus A. Anderson and the procedure has been published;<sup>5</sup> all other thiols used were commercially available and were used as received. Self-assembled monolayers (SAMs) of thiols are formed spontaneously upon exposure the gold electrode (either roughened or polished and annealed as described above) to a solution of the thiol in EtOH.<sup>6</sup> Prior to immersion, the gold electrodes were rinsed with EtOH to prevent contamination of thiol solutions with water adhered to the gold. The length of the exposure did not affect any of the results in these studies and times between 30 min and 24 hours were used as convenient. Thiol concentrations were 0.5 mM for AMT only, 0.5 mM AMT + 1.5 mM ethanethiol (ET) for

AMT/ET mixed monolayers, and 1 mM for all other thiols. It should be noted that AMT is not entirely soluble in EtOH, so this leads to some uncertainty regarding the actual AMT concentrations in solution. AMT is soluble in THF and THF/EtOH mixtures, but these solutions did not lead to SAM formation. The modified electrodes were rinsed with EtOH to remove any excess thiols.

#### *Laccase Purification and Electrode Modification*

Laccase from *Trametes versicolor* (*TvLc*) was purchased from Aldrich and purified by Nicholas M. Marshall and Bryant E. Kearl using a method modified from previously published protocols that is described elsewhere.<sup>5,7-8</sup> The activity of the provided *TvLc* solution was found to be >500 U/mL by UV-VIS spectroscopy using 3 mM ABTS as the substrate, the unit U corresponds to the oxidation of 1  $\mu$ mol ABTS per minute. The use of high-purity *TvLc* solutions is critical to obtain active electrodes. Gold electrodes modified with either AMT or AMT/ET as described above were rinsed with EtOH and immersed in a diluted *TvLc* solution prepared from 30  $\mu$ L of the >500 U/mL *TvLc* stock solution and 2970  $\mu$ L of pH 4.0 citrate-phosphate buffer. The electrode was allowed to soak for 1 h at ambient temperature prior to use (or could be soaked 24 h at 5  $^{\circ}$ C without any difference in activity). The electrode was rinsed with copious amounts of water to remove unbound Lc prior to prompt transfer to the electrochemical cell. If the surface is allowed to dry, all *TvLc* activity is lost.

#### **Carbon Working Electrode Preparation**

##### *Preparation of Cu(DAT) Modified Carbon Black<sup>9</sup>*

Carbon black (Vulcan XC-72, Cabot) (1.00 g),  $\text{Cu}(\text{SO}_4)_2 \cdot 5\text{H}_2\text{O}$  (Aldrich, 99.995%) (0.200 g, 0.801 mmol), and water (Milli-Q UV Plus, 18.2 M $\Omega$ ) (20 mL) were

combined and sonicated to form a viscous suspension. A solution of 3,5-diamino-1,2,4-triazole (DAT) (Aldrich, 98%) (0.159 g, 1.60 mmol) in water (10 mL) was then added drop-wise with stirring. After the mixture was stirred for 18 h, the solids were collected by suction filtration and dried in vacuo for 3 h at 90 °C, and then pulverized with a mortar and pestle. Elemental Analysis (%) found: C 85.2, H 0.14, N 5.36, and Cu 3.76.

#### *Preparation of Fe/N/C Electrocatalysts<sup>10</sup>*

To prepare carbon supported iron phthalocyanine (FePc), 20.0 mg of iron(II) phthalocyanine (Aldrich, 90%) were suspended in 10 mL of concentrated sulfuric acid, 0.50 g of Vulcan XC-72 was added and the mixture was sonicated for 2 h. The suspension was then poured into water and the solids were collected by suction filtration, rinsed with water, and dried under vacuum at 90 °C overnight. To prepare pyrolyzed FePc, carbon supported FePc was placed in a quartz boat in a quartz tube furnace under a 50 mL/min flow of Ar, the temperature was ramped to 800 °C over the course of 10 min, held at 800 °C for 20 min, and then allowed to cool to room temperature over the course of 3 h. A mass loss of 3.6% occurred during pyrolysis.

#### *Drop-casting Electrocatalyst Inks onto Glassy Carbon Working Electrodes<sup>10-11</sup>*

Working electrodes consisted of 5 mm diameter glassy carbon disks in Teflon holders (Pine Research Instrumentation) which were mechanically polished by hand using alumina suspensions in ultrapure water (0.05 µm, Buehler) on MicroCloth<sup>®</sup> disks (Buehler) adhered to a flat glass plate and then sonicated in ultrapure water to remove the excess alumina. For rotating ring-disk electrode studies, the glassy carbon disk was removed and polished separately from the Pt ring. Electrocatalyst inks were (re)suspended by sonication and then applied to the glassy carbon disk and allowed to dry. For CuDAT, the ink contained 1.0 mg mL<sup>-1</sup> carbon-supported catalyst and 4 µL mL<sup>-1</sup>

Nafion<sup>®</sup> (Aldrich, 5% solution) in water, and a 20  $\mu\text{L}$  drop was applied to the electrode and dried under a stream of Ar (the flow rate was adjusted until a uniform catalyst distribution was obtained). For FePc and pyrolyzed FePc, the inks contained 10 mg of carbon-supported catalyst and 95  $\mu\text{L}$  of Nafion<sup>®</sup> in 350  $\mu\text{L}$  of ethanol, a 7  $\mu\text{L}$  drop was applied to the electrode and air dried under an inverted beaker.<sup>12</sup> Between consecutive measurements with the same catalyst, the old catalyst was removed with isopropyl alcohol and a Kimwipe and fresh catalyst was applied without re-polishing.

### **Electrochemical Measurements**

Electrochemical measurements were performed in a standard three electrode configuration (or four electrode configuration for rotating ring-disk electrode studies) using a CHI 760C or CHI 760D bipotentiostat (CH Instruments). For rotating disk electrode (RDE) studies, a modulated speed rotator (model MSRX or AFMSRCE, Pine Research Instrumentation) was used. For studies on gold the working electrode was placed in hanging meniscus contact with the electrolyte. For studies on carbon the electrode was held in a Teflon holder. A Pt gauze counter electrode was separated from the working electrode by a porous glass frit and a “no leak” Ag/AgCl reference electrode (Cypress Systems) was isolated with a Luggin capillary. The reference electrode was calibrated to the reversible hydrogen electrode (RHE) by sparging the cell with H<sub>2</sub> and measuring the open circuit potential (OCP) at a Pt working electrode. The headspace of the cell was closed and either Ar or O<sub>2</sub> atmospheres were maintained during experiments with a slight positive pressure generated by a water or oil filled bubbler on the gas outlet from the cell.

## **Magnetic Measurements<sup>9</sup>**

Magnetic susceptibility data were kindly provided by Amber C. McConnell, William W. Shum, and Prof. Joel S. Miller (University of Utah). The 5 to 300 K magnetic susceptibility of Cu(DAT) on Vulcan was measured on a Quantum Design MPMS-5XL magnetometer. In order to correct for the diamagnetism of the carbon support, the susceptibility of unmodified Vulcan XC-72 was also measured across the entire temperature range and then subtracted.

## **Probe Microscopy<sup>5</sup>**

Scanning tunneling microscopy (STM) was performed by Jeremy J. Hatch. STM measurements were carried out using a Nanoscope III E (Digital Instruments). The gold substrate was clamped to the stage using a Teflon cell. Pt-Ir STM tips (0.25 mm in diameter) were purchased from Veeco Instruments. Atomic force microscopy (AFM) was performed by Andrew S. Campbell. AFM images were collected in contact mode using a PicoSPM 300 atomic force microscope (Agilent Technologies) controlled with a Nanoscope E controller unit (Digital Instruments, now Veeco). Contact-mode cantilevers ( $\text{Si}_3\text{N}_4$  with a reflective gold coating) were rinsed with EtOH and dried in air under UV before use. Scan sizes were varied between 164 nm (Z range = 50 nm) and 4.0  $\mu\text{m}$  (Z range = 600 nm) to ensure that all features were within the scan range. All experiments were run in air under ambient conditions.

## References

- (1) Britton, H. T. S.; Robinson, R. A., CXCVIII.-Universal Buffer Solutions and the Dissociation Constant of Veronal. *J. Chem. Soc.* **1931**, 1456-1462.
- (2) Batina, N.; Dakkouri, A. S.; Kolb, D. M., The Surface Structure of Flame-Annealed Au(100) in Aqueous Solution: An STM Study. *J. Electroanal. Chem.* **1994**, *370*, 87-94.
- (3) Gao, P.; Gosztola, D.; Leung, L.-W. H.; Weaver, M. J., Surface-Enhanced Raman Scattering at Gold Electrodes: Dependence on Electrochemical Pretreatment Conditions and Comparisons with Silver. *J. Electroanal. Chem.* **1987**, *233*, 211-222.
- (4) Liu, Y.-C.; Hwang, B.-J.; Jian, W.-J., Effect of Preparation Conditions for Roughening Gold Substrate by Oxidation-Reduction Cycle on the Surface-Enhanced Raman Spectroscopy of Polypyrrole. *Mater. Chem. Phys.* **2002**, *73*, 129-134.
- (5) Thorum, M. S.; Anderson, C. A.; Hatch, J. J.; Campbell, A. S.; Marshall, N. M.; Zimmerman, S. C.; Lu, Y.; Gewirth, A. A., Direct, Electrocatalytic Oxygen Reduction by Laccase on Anthracene-2-Methanethiol-Modified Gold. *J. Phys. Chem. Lett.* **2010**, *1*, 2251-2254.
- (6) Tour, J. M.; Jones, L.; Pearson, D. L.; Lamba, J. J. S.; Burgin, T. P.; Whitesides, G. M.; Allara, D. L.; Parikh, A. N.; Atre, S., Self-Assembled Monolayers and Multilayers of Conjugated Thiols,  $\alpha,\omega$ -Dithiols, and Thioacetyl-Containing Adsorbates. Understanding Attachments between Potential Molecular Wires and Gold Surfaces. *J. Am. Chem. Soc.* **1995**, *117*, 9529-9534.
- (7) Hudak, N. S.; Gallaway, J. W.; Barton, S. C., Formation of Mediated Biocatalytic Cathodes by Electrodeposition of a Redox Polymer and Laccase. *J. Electroanal. Chem.* **2009**, *629*, 57-62.
- (8) Blanford, C. F.; Heath, R. S.; Armstrong, F. A., A Stable Electrode for High-Potential, Electrocatalytic O<sub>2</sub> Reduction Based on Rational Attachment of a Blue Copper Oxidase to a Graphite Surface. *Chem. Commun.* **2007**, 1710-1712.
- (9) Thorum, M. S.; Yadav, J.; Gewirth, A. A., Oxygen Reduction Activity of a Copper Complex of 3,5-Diamino-1,2,4-Triazole Supported on Carbon Black. *Angew. Chem., Int. Ed.* **2009**, *48*, 165-167.
- (10) Thorum, M. S.; Hankett, J. M.; Gewirth, A. A., Poisoning the Oxygen Reduction Reaction on Carbon-Supported Fe and Cu Electrocatalysts: Evidence for Metal-Centered Activity. *J. Phys. Chem. Lett.* **2011**, *2*, 295-298.

- (11) Brushett, F. R.; Thorum, M. S.; Lioutas, N. S.; Naughton, M. S.; Tornow, C.; Jhong, H. R.; Gewirth, A. A.; Kenis, P. J. A., A Carbon-Supported Copper Complex of 3,5-Diamino-1,2,4-Triazole as a Cathode Catalyst for Alkaline Fuel Cell Applications. *J. Am. Chem. Soc.* **2010**, *132*, 12185-12187.
- (12) Birry, L.; Zagal, J. H.; Dodelet, J.-P., Does CO Poison Fe-Based Catalysts for ORR? *Electrochem. Commun.* **2010**, *12*, 628-631.

### CHAPTER 3. Direct, Electrocatalytic Oxygen Reduction by Laccase on Anthracene-2-methanethiol-Modified Gold

*Adapted with permission from The Journal of Physical Chemistry Letters, 2010, 1, pp 2251-2254. Copyright © 2010 American Chemical Society. Cyrus A. Anderson synthesized and provided anthracene-2-methanethiol. Jeremy J. Hatch performed scanning tunneling microscopy and provided Figure 3.3. Andrew S. Campbell performed atomic force microscopy and provided Figure 3.5. Nicholas M. Marshall and Bryant E. Kearl provided purified laccase.*

Although the 4 e<sup>-</sup> electroreduction of dioxygen to water is highly favored thermodynamically with a reversible reduction potential of 1.23 V versus the reversible hydrogen electrode (RHE), this potential is rarely realized because the reaction is kinetically slow and proceeds only at significant overpotentials (ca. -300 mV) even with the best Pt-based catalysts. The slow kinetics of the oxygen reduction reaction (ORR) is one of the major fundamental challenges to the widespread application of fuel cells and electrocatalysis of the ORR is the subject of extensive research efforts.<sup>1</sup>

Some multicopper oxidases, particularly certain types of laccase (Lc), reduce O<sub>2</sub> at significantly smaller overpotentials than Pt and have been utilized as cathode electrocatalysts in enzyme-based fuel cell applications.<sup>2</sup> Lc functions as an electrocatalyst on carbon electrodes as it adsorbs in an orientation that allows direct electron transfer (DET) from the electrode to a type 1 (T1) Cu site; subsequent internal electron transfer transports the electron to a mixed type 2/type 3 (T2/T3) tricopper cluster where O<sub>2</sub> is activated and reduced.<sup>3</sup> Although poor durability and low current densities are typical, significant improvements are realized upon diazonium modification of graphite and high surface area carbon electrodes to incorporate anthracene moieties on the surface prior to



the adsorption of Lc.<sup>4-5</sup> Anthracene purportedly mimics a natural substrate of the enzyme and penetrates the hydrophobic pocket near the T1 Cu site which properly orients the enzyme on the surface, facilitates electron transfer to the T1 Cu site, and reduces dissolution of enzyme off of the electrode surface. A key parameter in the characterization of electrocatalysts is the slope of a Tafel plot; however Lc-modified carbon electrodes exhibit nonlinear Tafel behavior.<sup>4</sup> Characterization of Lc on a better defined noble metal surface such as Au is desired to provide a potentially superior analytical platform.

On Au, Lc does not adsorb in the proper orientation for direct electrocatalysis at low overpotentials.<sup>3</sup> Prior investigations of Lc on Au electrodes investigated a variety of strategies including adsorption of the enzyme to bare and to thiol-modified Au and covalent attachment to thiol-modified Au.<sup>3, 6-10</sup> However none of these motifs allowed observation of the direct electrocatalytic reduction of O<sub>2</sub> at low overpotentials. Direct electrocatalysis has been reported for a low potential (high overpotential) Lc.<sup>11</sup> Recently, it was also reported that adsorption of Lc to 50 nm Au nanoparticles allows the observation of direct electrocatalysis.<sup>12</sup> Herein we report that modification of a roughened Au surface with anthracene-2-methanethiol (AMT) to orient and bind Lc from *Trametes versicolor* (TvLc) enables the direct electrocatalytic reduction of O<sub>2</sub> at low overpotentials (see Figure 3.1). Additionally, we report the successful observation of linear Tafel behavior.

A self-assembled monolayer (SAM) of AMT on polished Au was characterized electrochemically and by scanning tunneling microscopy (STM). The Fe(CN)<sub>6</sub><sup>3-</sup>/Fe(CN)<sub>6</sub><sup>4-</sup> redox couple was inhibited on an AMT modified Au electrode

relative to a clean Au electrode (Figure 3.2) consistent with the formation of a barrier type film that allows a small residual current to pass.<sup>13</sup> As seen in Figure 3.3, a hexagonal closest packed overlayer is formed by the AMT on the Au(poly) surface with nearest-neighbor spacing of *ca.* 0.4 nm. Similarly,  $(\sqrt{3} \times \sqrt{3})R30^\circ$  lattices of benzyl mercaptan and 4-biphenylmethanethiol monolayers form on Au(111) surfaces with nearest-neighbor spacing of  $0.49 \pm 0.01$  nm.<sup>14</sup> On the basis of theoretical work done by Sellers *et al.*, the methylene spacer likely promotes a vertical geometry allowing for strong intermolecular interactions between the AMT molecules.<sup>15</sup> However, isolated anthracene moieties need to protrude from the surface in order to access the hydrophobic pocket of Lc and orient the enzyme. Indeed, we found that the ORR activity of TvLc at a polished Au electrode modified with an AMT SAM was not significant, and was comparable to prior observations made with other thiols (see Figure 3.4).

To disrupt the SAM and create isolated anthracene moieties accessible to the enzyme we electrochemically roughened the Au surface forming rounded asperities on the order of *ca.* 100 nm in diameter as observed by atomic force microscopy (AFM) (Figure 3.5). TvLc adsorbed on the roughened Au surface modified with AMT exhibited direct electrocatalytic reduction of O<sub>2</sub> at potentials approaching 1 V vs. RHE (Figure 3.6). Use of a mixed monolayer of AMT and ethanethiol (ET) on a roughened surface (see Figure 3.1) increased the onset of the ORR to 1.13 V versus RHE and yielded current densities approaching  $-25 \mu\text{A}/\text{cm}^2$  in quiescent solution (Figure 3.6). We attribute the improved activity to the formation of an increased number of anthracene moieties accessible to TvLc in the mixed monolayer.

In the absence of O<sub>2</sub>, there is no Faradaic contribution to the voltammetry of roughened Au electrodes modified with AMT/ET and TvLc in the potential window examined (Figure 3.6). Based on the electrocatalytic current densities, we can estimate that the expected current density from e<sup>-</sup> transfer to the Cu sites in the absence of O<sub>2</sub> is too small to observe because of the low surface concentration of TvLc due to the low number of accessible anthracene moieties, even with roughening and utilization of a mixed monolayer. The rate constant for O<sub>2</sub> binding to the tricopper site has been found to be  $2 \times 10^6 \text{ M}^{-1} \text{ s}^{-1}$  and must be equal to (or greater) than the rate constant for the rate determining step (RDS) for the overall oxygen reduction reaction.<sup>16</sup> Multiplication by 4 e<sup>-</sup> for each turn-over of the enzyme, the concentration of dissolved O<sub>2</sub> (*ca.* 1 mM), and Faraday's constant (96500 C/mol) yields a maximum electrocatalytic current of  $8 \times 10^8 \text{ A}$  per mol Lc. Division of this number into the maximum observed electrocatalytic current density ( $25 \text{ } \mu\text{A cm}^{-2}$ ) yields a maximum TvLc surface concentration of  $3 \times 10^{-14} \text{ mol cm}^{-2}$  equivalent to  $1.2 \times 10^{-13} \text{ mol Cu cm}^{-2}$ . The peak current density ( $j_p$ ) expected for voltammetry of a Nernstian adsorbate layer is given by Equation 3.1

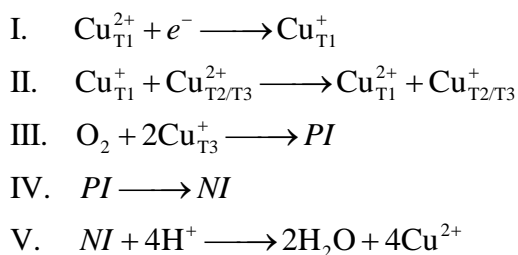
$$j_p = (9.39 \times 10^5) n^2 v \Gamma \quad (3.1)$$

where  $n$  is number of e<sup>-</sup> transferred (1),  $v$  is the scan rate ( $5 \text{ mV s}^{-1}$ ), and  $\Gamma$  is the surface concentration of the adsorbate ( $1.2 \times 10^{-13} \text{ mol Cu cm}^{-2}$ ).<sup>17</sup> The upper bound for  $j_p$  in our case is therefore  $0.6 \text{ nA cm}^{-2}$ , several orders of magnitude smaller than the capacitive charging current in the voltammogram ( $300 \text{ nA cm}^{-2}$ ) and also smaller than the noise in the measurement ( $2 \text{ nA cm}^{-2}$ ).

Figure 3.6 also shows data obtained at a roughened electrode modified with hexadecanethiol (HDT) in place of AMT; the absence of O<sub>2</sub> reduction currents indicates

that the anthracene moiety is required to orient the enzyme properly. Electrodes prepared with *TvLc* on roughened gold without a thiol modification, or modified with benzyl mercaptan, also did not show any significant ORR activity (Figure 3.7).

Tafel plots of the ORR at the electrodes utilizing AMT only and the AMT/ET mixture to bind *TvLc* have linear regions with a slope of  $\sim 144$  mV/dec (Figure 3.8). The similar slope in both systems indicates that the ORR mechanism does not change as a function of the number of active *TvLc* sites on the electrode surface. *TvLc* reduces oxygen following a ping-pong-type mechanism that couples the single electron oxidation of four substrate molecules to the four electron reduction to water as represented below



where *PI* and *NI* designate the peroxy intermediate and native intermediate respectively.<sup>16</sup>

For a multistep multielectron reaction, the relationship between the transfer coefficient ( $\alpha$ ) and the reaction mechanism is described by Equation 3.2

$$\alpha = \left( \frac{\gamma}{\nu} + r\beta \right) \quad (3.2)$$

where  $\gamma$  is the number of electrons transferred prior to the RDS,  $\nu$  is the stoichiometric number (the number of times the step occurs per cycle of the overall reaction),  $r$  is the number of electrons transferred during the RDS, and  $\beta$  is the symmetry factor (usually  $\sim 0.5$ ).<sup>18</sup> If step I (the outer sphere single electron transfer from the electrode to the T1 Cu site) is the RDS, then  $\gamma = 0$  and  $r = 1$ ; therefore  $\alpha = \beta$ . If step II is the RDS,

then  $\gamma = 4$ ,  $\nu = 3$ , and  $r = 0$ ; therefore  $\alpha = 4/3$ . If any of steps III through V are the RDS, then  $\gamma = 4$ ,  $\nu = 1$ , and  $r = 0$ ; therefore  $\alpha = 4$ . The value of  $\alpha$  is determined from the Tafel slope using Equation 3.3.<sup>18</sup>

$$\frac{dE}{d \log i} = \frac{2.3RT}{\alpha F} \quad (3.3)$$

The observed Tafel slope of 144 mV/dec yields  $\alpha = 0.41$  which is most consistent with step I as the RDS and  $\alpha = \beta = 0.41$ , which is within the normal range expected for the symmetry factor. This is consistent with the suggestion that the first electron transfer is the RDS for the oxidation of certain substrates with Lc (based on the observation that the catalytic efficiency of various laccases depends on the redox potential of the T1 Cu site).<sup>3</sup> It also illustrates the remarkable ability of the tricopper T2/T3 site to activate the O=O bond, the typical RDS with other electrocatalysts (including Pt).<sup>1</sup>

Linear Tafel behavior is expected only when current densities at overpotentials greater than *ca.* 118 mV are free from mass-transport effects.<sup>17</sup> Thus, the Tafel plot of the electrode with AMT only is more linear than the electrode with the AMT/ET mixture, and the still higher geometric current density *Tv*Lc-modified carbon electrodes reported by Blanford et al. do not have linear Tafel behavior.<sup>4</sup> The lack of linearity may be due to mass-transport effects accompanying the higher current densities, or the heterogeneous nature of the carbon surface.

The observation of linear Tafel behavior from laccase on a modified Au surface provides an analytical platform with which to further characterize different laccase systems. Whereas our system is suitable for the characterization of Lc at a Au surface, systems employing high surface area carbons remain at this time more practical for enzyme based fuel cells because of the accessibility of higher current densities.

Optimization of laccase binding site density on Au may provide for further increases in current density in the future.

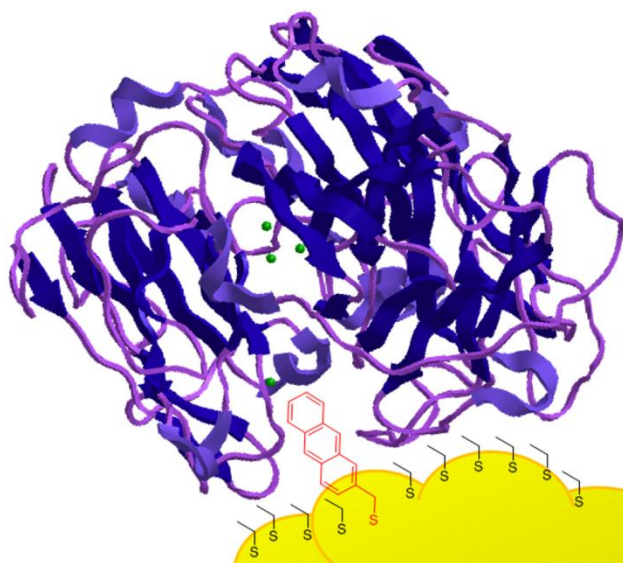


**Figure 3.1.** Schematic representation of Lc from *Trametes versicolor* properly oriented for electrocatalytic reduction of  $O_2$  at an electrochemically roughened Au surface modified with a mixture of anthracene-2-methanethiol (AMT) and ethanethiol (ET). The AMT is shown in the hydrophobic pocket where it facilitates electron transfer from the electrode surface to the T1 Cu site. After an internal electron transfer, the  $4 e^-$  reduction of  $O_2$  to water occurs at the T2/T3 tricopper cluster near the center of the enzyme.<sup>19</sup>

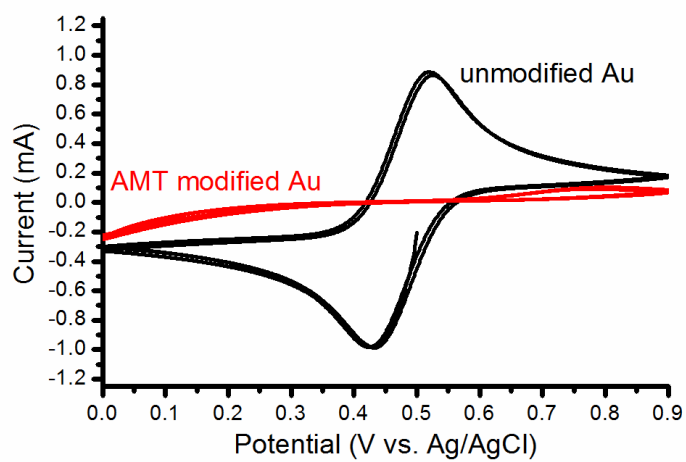


**Figure 3.2.** Cyclic voltammograms of 10 mM  $\text{K}_3\text{Fe}(\text{CN})_6$  at a polished, unmodified Au working electrode (black) and a Au working electrode modified with AMT (red) recorded in 0.5 M  $\text{Na}_2\text{SO}_4$  sparged with Ar at 50 mV/s.



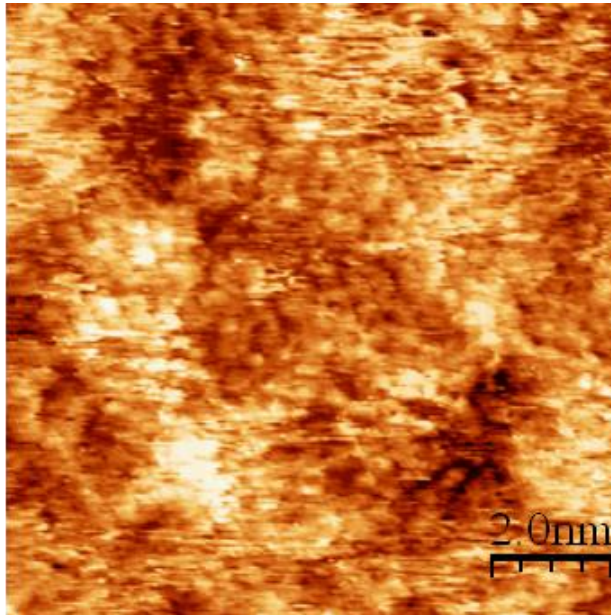


**Figure 3.3.** STM micrograph of hexagonal closest packed AMT monolayer formed on a polycrystalline Au surface. Nearest-neighbor spacing is ca. 0.4 nm within each domain. ( $V_{\text{bias}} = 150 \text{ mV}$ ,  $i_t = 2.00 \text{ nA}$ )

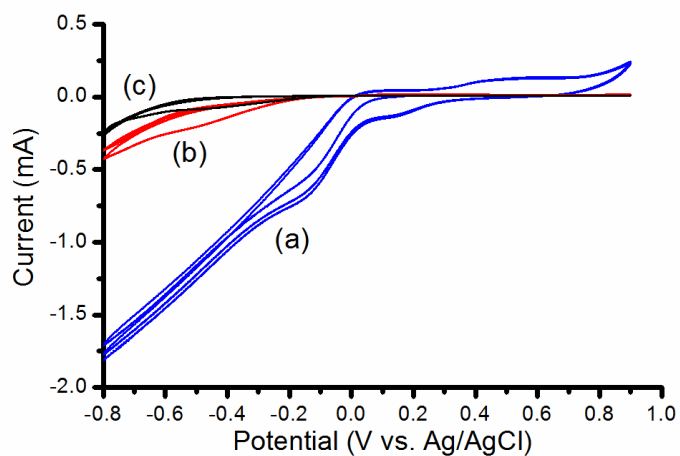


**Figure 3.4.** Cyclic voltammograms of clean Au (blue, curve a), AMT modified Au (red, curve b), and *TvLc* adsorbed on AMT modified Au (black, curve c) recorded in O<sub>2</sub> saturated pH 4.0 citrate buffer at 0.1 V/s. Working electrodes were 10 mm dia. polycrystalline Au disks polished to a mirror finish with 0.05 micron diamond slurries, sonicated in ultra-pure water, hydrogen flame annealed red hot for 10 min, and air cooled 8 min. AMT modified electrodes were immersed in a 0.5 mM AMT solution in EtOH 24h. *TvLc* modified electrodes prepared by immersing AMT modified electrode in 2 mL pH 4 citrate buffer with 40 $\mu$ L purified *TvLc* solution added for 1 h (extending exposure to 24 h had no effect on the voltammetry).

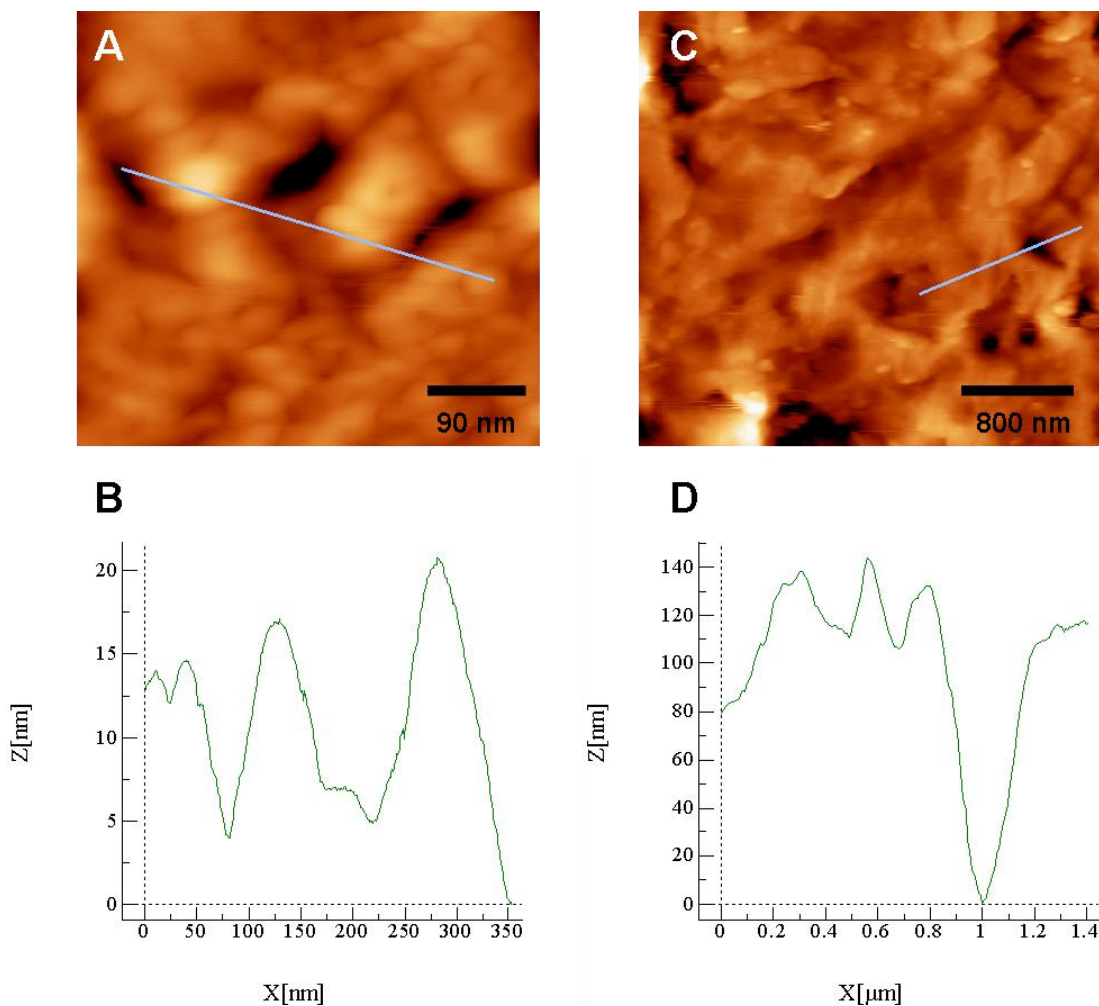


**Figure 3.5.** Atomic force micrographs (A, C) of an electrochemically roughened gold surface and corresponding cross-section traces (B, D) are shown. A 437 nm scan size (A) reveals small-scale features on the order of 3-20 nm in height. A larger, 4.0  $\mu\text{m}$  scan size (C) indicates larger-scale features of up to 120 nm as well as the smaller, 20 nm features observed in (A). Imaged in contact mode using a PicoSPM 300 atomic force microscope (Agilent Technologies) controlled with a Nanoscope E controller unit (Digital Instruments, now Veeco). Contact-mode cantilevers ( $\text{Si}_3\text{N}_4$  with a reflective gold coating) were rinsed with ethanol and dried in air under UV before use. Scan sizes were varied between 164 nm (Z range = 50 nm) and 4.0  $\mu\text{m}$  (Z range = 600 nm) to ensure that all features were within the scan range. All experiments were run in air under ambient conditions.

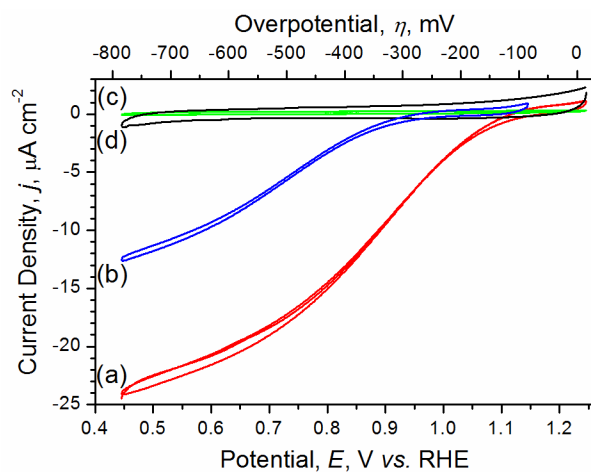


**Figure 3.6.** Cyclic voltammograms showing the electrocatalytic activity of *TvLc* adsorbed on a roughened Au electrode modified with: an AMT/ET mixture (red, curve a), AMT only (blue, curve b), and HDT (green, curve c) in  $O_2$  saturated electrolyte; and Lc on the AMT/ET modified electrode in Ar saturated solution (black, curve d). Data recorded at 5 mV/s in 0.1 M citric acid buffer adjusted to pH 4.00 with 0.2 M  $Na_2HPO_4$ .

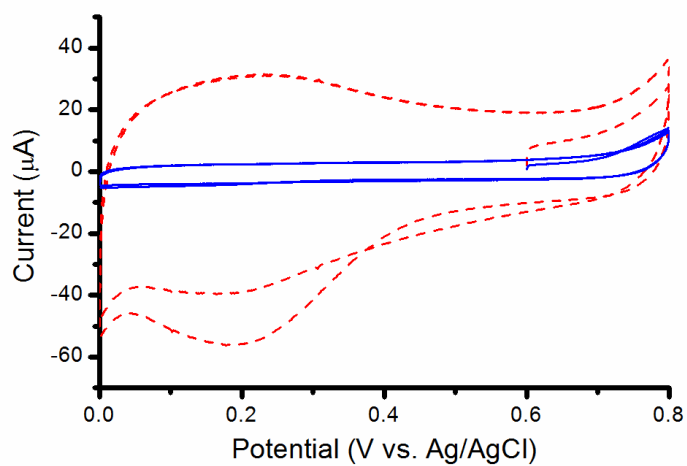


**Figure 3.7.** Cyclic voltammograms of *TvLc* adsorbed on electrochemically roughened Au electrodes with no thiol modification (dashed red) and modified with benzyl mercaptan (solid blue) recorded at 0.1 V/s in  $O_2$  saturated pH 4.0 citrate buffer.

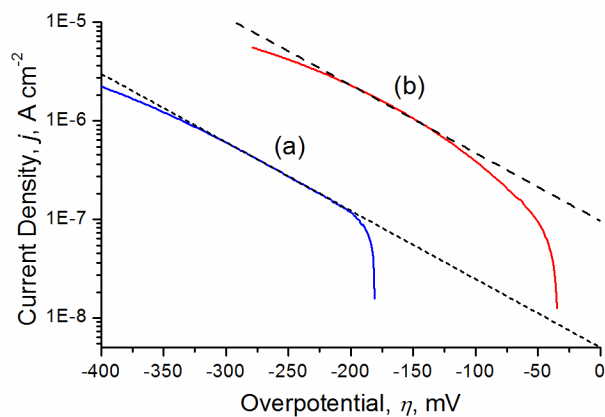


**Figure 3.8.** Tafel plots of the O<sub>2</sub> reduction activity of TvLc adsorbed on roughened Au electrodes modified with AMT (curve a, blue) and an AMT/ET mixture (curve b, red) in O<sub>2</sub> saturated pH 4.00 citrate-phosphate buffer; and linear fits equivalent to Tafel slopes of 144 mV/dec (short dashes) and 145 mV/dec (long dashes). Data recorded during a 5 mV/s cathodic potential scan.

## References

- (1) Gewirth, A. A.; Thorum, M. S., Electroreduction of Dioxygen for Fuel-Cell Applications: Materials and Challenges. *Inorg. Chem.* **2010**, *49*, 3557-3566.
- (2) Cracknell, J. A.; Vincent, K. A.; Armstrong, F. A., Enzymes as Working or Inspirational Electrocatalysts for Fuel Cells and Electrolysis. *Chem. Rev.* **2008**, *108*, 2439-2461.
- (3) Shleev, S.; Tkac, J.; Christenson, A.; Ruzgas, T.; Yaropolov, A. I.; Whittaker, J. W.; Gorton, L., Direct Electron Transfer between Copper-Containing Proteins and Electrodes. *Biosens. Bioelectron.* **2005**, *20*, 2517-2554.
- (4) Blanford, C. F.; Foster, C. E.; Heath, R. S.; Armstrong, F. A., Efficient Electrocatalytic Oxygen Reduction by the 'Blue' Copper Oxidase, Laccase, Directly Attached to Chemically Modified Carbons. *Faraday Discuss.* **2009**, *140*, 319-335.
- (5) Blanford, C. F.; Heath, R. S.; Armstrong, F. A., A Stable Electrode for High-Potential, Electrocatalytic O<sub>2</sub> Reduction Based on Rational Attachment of a Blue Copper Oxidase to a Graphite Surface. *Chem. Commun.* **2007**, 1710-1712.
- (6) Qiu, H.; Xu, C.; Huang, X.; Ding, Y.; Qu, Y.; Gao, P., Immobilization of Laccase on Nanoporous Gold: Comparative Studies on the Immobilization Strategies and the Particle Size Effects. *J. Phys. Chem. C* **2009**, *113*, 2521-2525.
- (7) Gallaway, J.; Wheeldon, I.; Rincon, R.; Atanassov, P.; Banta, S.; Barton, S. C., Oxygen-Reducing Enzyme Cathodes Produced from SLAC, a Small Laccase from *Streptomyces coelicolor*. *Biosens. Bioelectron.* **2008**, *23*, 1229-1235.
- (8) Klis, M.; Maicka, E.; Michota, A.; Bukowska, J.; Sek, S.; Rogalski, J.; Bilewicz, R., Electroreduction of Laccase Covalently Bound to Organothiol Monolayers on Gold Electrodes. *Electrochim. Acta* **2007**, *52*, 5591-5598.
- (9) Shleev, S.; Pita, M.; Yaropolov, A. I.; Ruzgas, T.; Gorton, L., Direct Heterogeneous Electron Transfer Reactions of *Trametes hirsuta* Laccase at Bare and Thiol-Modified Gold Electrodes. *Electroanalysis* **2006**, *18*, 1901-1908.
- (10) Pita, M.; Shleev, S.; Ruzgas, T.; Fernandez, V. M.; Yaropolov, A. I.; Gorton, L., Direct Heterogeneous Electron Transfer Reactions of Fungal Laccases at Bare and Thiol-Modified Gold Electrodes. *Electrochem. Commun.* **2006**, *8*, 747-753.
- (11) Johnson, D. L.; Thompson, J. L.; Brinkmann, S. M.; Schuller, K. A.; Martin, L. L., Electrochemical Characterization of Purified *Rhus vernicifera* Laccase: Voltammetric Evidence for a Sequential Four-Electron Transfer. *Biochemistry* **2003**, *42*, 10229-10237.

- (12) Dagys, M.; Haberska, K.; Shleev, S.; Arnebrant, T.; Kulys, J.; Ruzgas, T., Laccase - Gold Nanoparticle Assisted Bioelectrocatalytic Reduction of Oxygen. *Electrochem. Commun.* **2010**, *12*, 933-935.
- (13) Scharf, J.; Strehblow, H.-H.; Zeysing, B.; Terfort, A., Electrochemical and Surface Analytical Studies of Self-Assembled Monolayers of Three Aromatic Thiols on Gold Electrodes. *J. Solid State Electrochem.* **2001**, *5*, 396-401.
- (14) Tao, Y.-T.; Wu, C.-C.; Eu, J.-Y.; Lin, W.-L.; Wu, K.-C.; Chen, C.-H., Structure Evolution of Aromatic-Derivatized Thiol Monolayers on Evaporated Gold. *Langmuir* **1997**, *13*, 4018-4023.
- (15) Sellers, H.; Ulman, A.; Shnidman, Y.; Eilers, J. E., Structure and Binding of Alkanethiolates on Gold and Silver Surfaces: Implications for Self-Assembled Monolayers. *J. Am. Chem. Soc.* **1993**, *115*, 9389-9401.
- (16) Solomon, E.; Sarangi, R.; Woertink, J.; Augustine, A.; Yoon, J.; Ghosh, S., O<sub>2</sub> and N<sub>2</sub>O Activation by Bi-, Tri-, and Tetranuclear Cu Clusters in Biology. *Acc. Chem. Res.* **2007**, *40*, 581-591.
- (17) Bard, A. J.; Faulkner, L. R., *Electrochemical Methods: Fundamentals and Applications*. Wiley: New York, 2001.
- (18) Bockris, J. O. M.; Reddy, A. K., *Modern Electrochemistry*. Plenum Press: New York, 1973; Vol. 2.
- (19) Piontek, K.; Antorini, M.; Choinowski, T., Crystal Structure of a Laccase from the Fungus *Trametes versicolor* at 1.90 Å Resolution Containing a Full Complement of Coppers. *J. Biol. Chem.* **2002**, *277*, 37663-37669.



## CHAPTER 4. Oxygen Reduction Activity of a Copper Complex with 3,5-Diamino-1,2,4-triazole Supported on Carbon Black

*Adapted with permission from Angewandte Chemie International Edition, 2009, 48, pp 165–167. Copyright © 2009 Wiley-VCH Verlag GmbH & Co. KGaA, Weinheim. Magnetic susceptibility data (Figure 4.6) were kindly provided by Amber C. McConnell, William W. Shum, and Prof. Joel S. Miller (University of Utah).*

Electrocatalysis of the oxygen reduction reaction (ORR) is currently of widespread interest due to its application in fuel cell cathodes. Slow reaction kinetics significantly impact the efficiency of fuel cells and, even with Pt catalysts, the onset of the ORR occurs at approximately 1.0 V, which is well below the reversible potential for oxygen reduction of 1.23 V versus the reversible hydrogen electrode (RHE).<sup>1</sup> Multicopper oxidases (exemplified by laccase) activate oxygen at a site containing three Cu atoms with spacings of approximately 3.5 Å and exhibit remarkable ORR electroactivity at potentials approaching 1.2 V (versus RHE).<sup>2-3</sup> Given the high cost and limited supply of Pt, a copper-containing complex adsorbed on an electrode surface that exhibited this level of reactivity would be highly desirable.

There are few reports of synthetic copper complexes that exhibit significant ORR activity. Several mononuclear Cu complexes have been investigated via adsorption onto graphite electrodes.<sup>4-9</sup> Copper(II) complexes with phenanthroline ligands, which were popularized by Zhang and Anson,<sup>6</sup> are the best-studied to date. McCrory et al. have investigated the copper complexes of a variety of substituted phenanthrolines, the best of which demonstrated an ORR onset of about 0.68 V (RHE) at pH 4.8, and concluded that further increases in activity were unlikely with this system.<sup>7</sup> Attempts that used putative

multicopper complexes include a water soluble catalyst formed by the coordination of two copper(II) ions in a hexaazamacrocyclic ligand,<sup>10</sup> and electrodes modified with solution-cast polymers containing copper(II) ions, including a copper–poly(histidine) complex,<sup>11</sup> and a polymeric copper(II) oxalato complex.<sup>12</sup> However, the demonstration of polynuclearity when adsorbed on an electrode in any of these systems is lacking. A cytochrome *c* oxidase model compound with a Cu–Fe site has also been investigated by adsorption onto graphite, but the ORR onset is quite low at about 0.2 V versus RHE and the complex that contains only Fe has similar activity.<sup>13</sup>

The efficacy of laccase led us to wonder if Cu coordination complexes or polymers composed of Cu<sup>II</sup> coordinated with bridging azole-type ligands, such as the 3,5-diamino-1,2,4-triazole (DAT) ligand (Figure 4.1),<sup>14</sup> and with other weakly coordinated ligands (such as water or sulfate) might provide stability in addition to multicopper sites that could potentially bind and activate O<sub>2</sub> (as these have Cu···Cu spacings similar to laccase). The combination of aqueous solutions of CuSO<sub>4</sub> and a variety of substituted pyrazoles and triazoles leads to the precipitation of insoluble compounds. The lack of solubility was encouraging from a stability standpoint, but made them incompatible with the techniques previously used to prepare electrodes for electrochemical characterization which require the use of solution phases.<sup>4-13</sup>

Herein, we demonstrate a simple method for the evaluation of the electrocatalytic activity of insoluble coordination compounds by direct precipitation onto carbon black (Vulcan XC-72). Utilization of a carbon black support allows the use of electrode fabrication methods and characterization techniques developed for the analysis of carbon-supported Pt catalysts and could also facilitate the transition to practical application in a

fuel cell.<sup>1, 15</sup> We have applied this method to the evaluation of the ORR activity of the insoluble multi-Cu complex formed with 3,5-diamino-1,2,4-triazole (DAT).

Figure 4.2 shows the characterization of the Cu(DAT) complex supported on Vulcan and a blank sample of unmodified Vulcan using a rotating ring-disk electrode (RRDE) in an oxygen-saturated electrolyte at pH 7. The disk potential was swept to determine the potential dependence of the ORR and the ring potential was held constant at 1.2 V to observe the oxidation of any generated peroxide intermediate.<sup>15</sup> The collection efficiency of the ring under the conditions of the experiment was calculated to be 0.04 from the ring to disk current ratio obtained for the two electron reduction of oxygen by the unmodified Vulcan. This was used to calculate the fraction of peroxide formed with a method described elsewhere.<sup>15</sup> The onset of O<sub>2</sub> reduction occurs at a disk potential of 0.73 V (versus RHE) and the reduction current becomes diffusion-limited at approximately 0.35 V. At more negative values, the ring current is less than 1 μA, which corresponds to less than 5% peroxide intermediate generation or almost complete four electron reduction of O<sub>2</sub> to water. At more positive potentials the ring current increases until 50% peroxide intermediate formation is observed at approximately 0.7 V which corresponds to an average of three electrons per O<sub>2</sub>.

The steady-state oxygen reduction current was observed as a function of rotation rate at 0.0 V and at 0.5 V. The current is determined by the rate of mass transfer of oxygen to the electrode (which in turn is controlled via the rotation rate and is independent of the applied potential) and by the kinetics of the electron transfer process at the electrode surface (which is potential dependent). The combination of these effects is described by the Koutecký–Levich equation (Equation 4.1)<sup>16</sup>

$$\frac{1}{i} = \frac{1}{i_k} + \frac{1}{i_l} \quad (4.1)$$

where  $i_k$  is the kinetically controlled current (the current that would be observed when the rate of transport of oxygen to the electrode surface is much greater than the rate of reaction) and  $i_l$  is the diffusion-limited current (the current that would be observed when the rate of reaction is much greater than the rate of mass transport). The diffusion-limited current for a rotating disk is described by the Levich equation (Equation 4.2)<sup>16</sup>

$$i_l = 0.62nFAD_O^{2/3}\nu^{-1/6}C_O^*\omega^{1/2} \quad (4.2)$$

where  $n$  is the number of electrons transferred,  $F$  is Faraday's constant,  $A$  is the geometric surface area of the electrode (0.196 cm<sup>2</sup>),  $D_O$  is the diffusion coefficient of oxygen ( $1.7 \times 10^{-5}$  cm<sup>2</sup> s<sup>-1</sup>),  $\nu$  is the kinematic viscosity (0.01 cm<sup>2</sup> s<sup>-1</sup>),  $C_O$  is the bulk concentration of oxygen ( $1.3 \times 10^{-6}$  mol/cm<sup>3</sup>), and  $\omega$  is the angular velocity of the electrode (rad s<sup>-1</sup>).<sup>6</sup>

Plotting  $i^{-1}$  vs.  $\omega^{-1/2}$  at 0.0 V and 0.5 V leads to linear plots (Figure 4.3). The number of electrons transferred during the reaction at each potential can be calculated from the slopes and values of  $n = 3.8$  and  $n = 4.0$  are found at 0.0 V and 0.5 V respectively. The magnitude of the kinetic current corresponds to the inverse of the y-intercept. At 0.0 V the intercept is 0 indicating that the kinetic current is effectively infinite and the observed current is entirely diffusion limited at this potential. At 1600 rpm the magnitude of the diffusion limited current is found to be  $5.56 \pm 0.02$  mA cm<sup>-2</sup>. This corresponds to a value of  $n = 3.9$  using Equation (4.2). The diffusion limited current can be used in conjunction with Equation (4.1) to calculate the mass-transport-corrected kinetic current,  $i_k$ , throughout the potential range.

The catalyst is sufficiently stable to allow the evaluation of ORR activity over a wide range of pH values (Figure 4.4). The onset potential was found to increase linearly at a rate of 30 mV per pH unit of the electrolyte (Figure 4.4) which is equivalent to a -30 mV per pH unit change using a pH-independent reference. This is half the value of -60 mV per pH unit predicted by the Nernst equation for a reaction involving the transfer of one H<sup>+</sup> ion per electron and implies that the rate-determining step (RDS) involves the transfer of two electrons and one H<sup>+</sup> ion. This is consistent with either the reduction of two Cu<sup>II</sup> centers and the concomitant protonation of a bridging OH<sup>-</sup> or O<sup>2-</sup> ligand or with the reduction of O<sub>2</sub> to a hydroperoxo (HOO<sup>-</sup>) intermediate.

The observed ORR onset of 0.86 V (versus RHE) at pH 13 represents a reduction of the ORR overpotential to 0.37 V. To the best of our knowledge, this makes the Cu(DAT) complex the most efficient synthetic copper-based ORR electrocatalyst reported to date and the first to be evaluated at this pH value. The 0.73 V onset at pH 7 is higher than the 0.67 V onset reported for a Cu complex with a hexaazamacrocyclic ligand which was previously the highest onset reported at this or any pH.<sup>10</sup> At more acidic pH values the onset is comparable to the best mononuclear Cu phenanthroline complexes.<sup>7</sup>

The cycle-to-cycle reproducibility of Cu(DAT) at pH 7 was found to be excellent on the time scale of a typical experiment (10 min). Therefore, the stability was evaluated over a longer time scale (Figure 4.5). An initial 400 rpm RDE voltammogram had an onset potential ( $E_{\text{Onset}}$ ) of 0.74 V; a half-wave potential ( $E_{1/2}$ ) of 0.61 V; and a diffusion limited current ( $i_l$ ) of 2.8 mA cm<sup>-2</sup>. After being held at 0.1 V for 24 h,  $i_l$  decayed 4 % to 2.7 mA cm<sup>-2</sup>;  $E_{\text{Onset}}$  decreased slightly to 0.72 V and  $E_{1/2}$  decreased to 0.51 V. The electrode was then subjected to 100 potential cycles which resulted in larger decreases in

activity ( $i_l = 2.6$ ,  $E_{\text{Onset}} = 0.68$  V,  $E_{1/2} = 0.47$  V). At pH 1 and pH 13 there was a significant decline in activity upon repeated cycling of the applied potential likely due to instability of the complex at these pH values.

The two reported crystal structures containing Cu and the DAT ligand are consistent with the bridging coordination mode illustrated in Figure 4.1 and consistent with the ~1:1 ratio between Cu and DAT found by elemental analysis.<sup>14</sup> In order to characterize the adsorbed catalyst complex, magnetic susceptibility measurements were undertaken as shown in Figure 4.6. The expected value of  $\chi T$  for an  $S=1/2$  system is  $0.374 \text{ emu K mol}^{-1}$ , which is independent of the temperature and would indicate the presence of normal spin-only mononuclear Cu sites. The values of  $\chi T$  for the crystalline complexes of Cu with DAT increase with temperature, which is consistent with an antiferromagnetic interaction between  $\text{Cu}^{\text{II}}$  ions with a singlet ground state and a thermally populated triplet state.<sup>14</sup> For the adsorbed Cu(DAT) complex, we observe the expected low  $\chi T$  value at low temperature. This value increases with temperature to a peak value of  $0.372 \text{ emu K mol}^{-1}$  at 83 K, which implies that most of the Cu spins are effectively unpaired at this temperature. However, as the temperature is raised further there is a subsequent decrease in  $\chi T$  followed by a gradual increase to a value of  $0.283 \text{ emu K mol}^{-1}$  at 295 K. This complicated behavior indicates that the complex is distinct from those previously crystallized, but indicates that spin pairing between Cu centers occurs and that closely spaced Cu centers must be present.

The development of simple methods to adsorb insoluble Cu complexes on carbon black opens the possibility of developing other catalysts more closely aligned to the three Cu active site of laccase. It also allows the use of ex situ methods to characterize and

obtain structural information about the on-electrode catalyst. The observed ORR activity of the Cu(DAT) complex is very high for synthetic copper-based electrocatalysts and, given the demonstrated activity of laccase, we believe large increases in activity may be realized upon the development of improved model complexes.

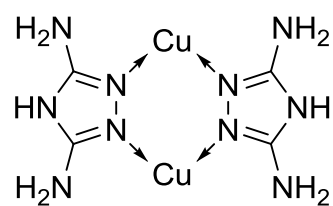


**Figure 4.1.** 3,5-diamino-1,2,4-triazole (DAT) ligands bridging two copper centers. Typical Cu...Cu spacing is 3.5 Å. Counter-ions and ligated water are omitted for clarity.



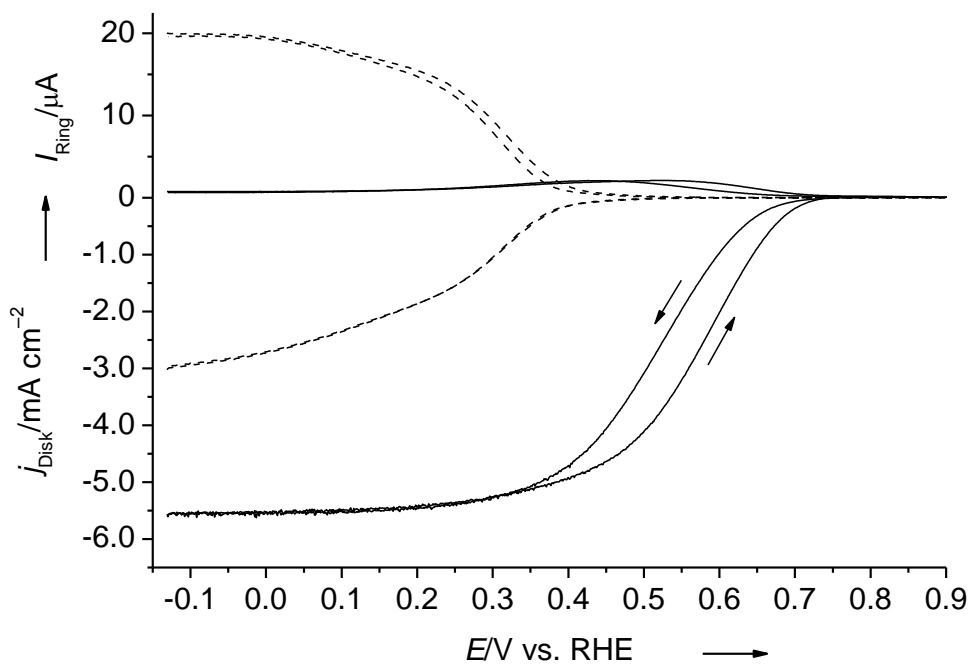


**Figure 4.2.** Reduction of  $\text{O}_2$  at a rotating Pt ring/glassy carbon disk electrode supporting Cu(DAT)/Vulcan (solid line) or unmodified Vulcan XC-72 (dashed line) at 1600 rpm in  $\text{NaClO}_4$  (0.1 M) and Britton–Robinson Buffer (0.04 M, pH 7.0) saturated with  $\text{O}_2$ . Disk current density ( $j_{\text{disk}}$ ) is shown on the lower half and ring current ( $I_{\text{ring}}$ ) is shown on the upper half of the y-axis. The disk potential was scanned at 5 mV/s; the ring potential was constant at 1.2 V.

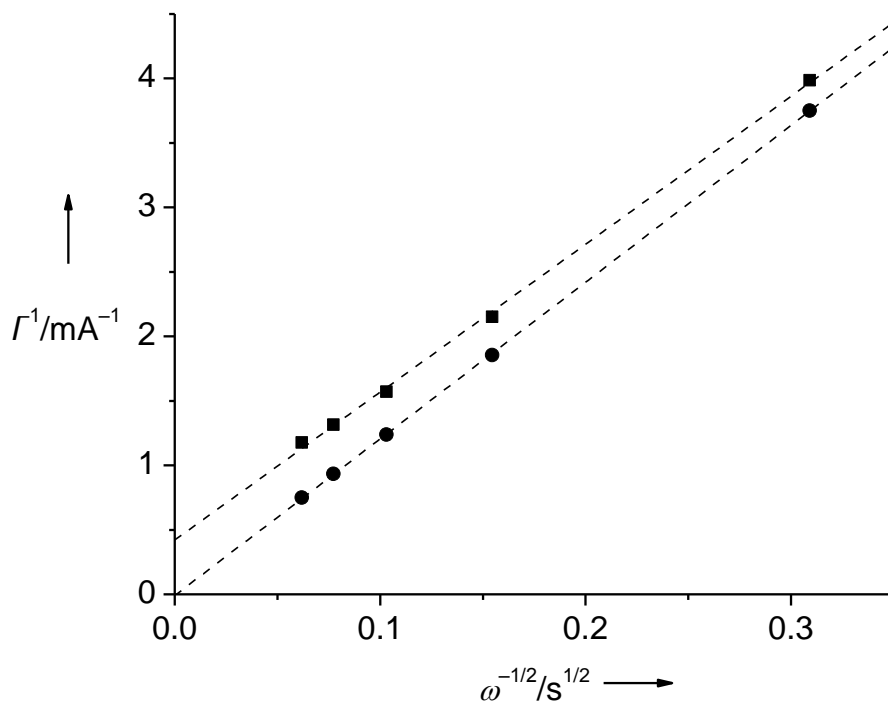


**Figure 4.3.** Koutecký–Levich plots of the inverse of the steady state oxygen reduction current at 0.0 V (circles) and 0.5 V (squares) versus the inverse square root of the electrode rotation rate with linear fits. The number of electrons transferred during the reaction,  $n$ , calculated from these slopes is 3.8 at 0.0 V and 4.0 at 0.5 V.

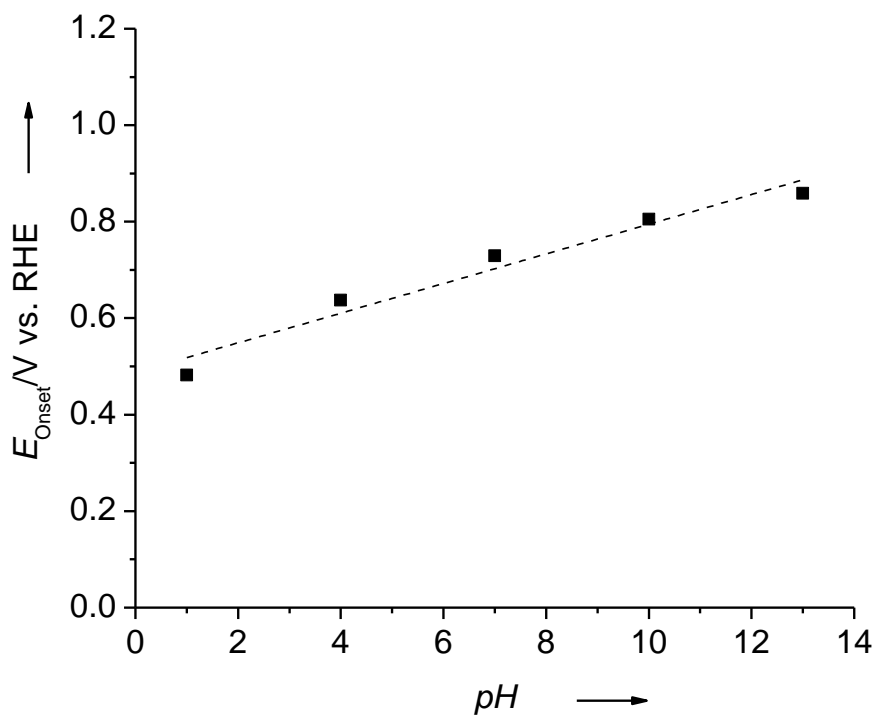


**Figure 4.4.** Potentials at which the onset of  $\text{O}_2$  reduction occurs at electrodes modified with Cu(DAT) in electrolytes of varying pH and a linear fit ( $31 \pm 4$  mV per pH unit slope and  $0.49 \pm 0.03$  V y-intercept). Electrodes were rotated at 1600 rpm in either  $\text{HClO}_4$  (0.1 M);  $\text{NaClO}_4$  (0.1 M) and Britton–Robinson buffers (0.04 M, pH 4, 7, 10); or  $\text{NaOH}$  (0.1 N) saturated with  $\text{O}_2$ . Potential scanned at 5 mV/s. Onset potential chosen as the potential at which the current density reaches  $-5 \mu\text{A cm}^{-2}$ .

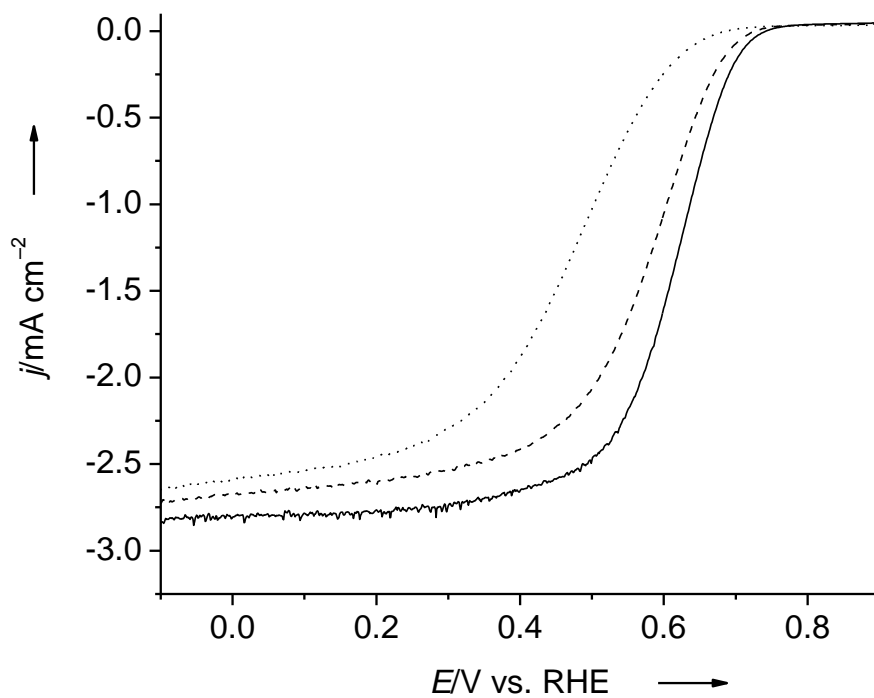


**Figure 4.5.** Reduction of  $\text{O}_2$  at a rotating glassy carbon disk electrode supporting Cu(DAT)/Vulcan. Scans were recorded after the electrode was freshly prepared (solid line), then held at 0.1 V for 24 h (dashed line), and subsequently cycled 100 times (dotted line) at 400 rpm in  $\text{NaClO}_4$  (0.1 M) and Britton–Robinson buffer (0.04 M, pH 7.0) saturated with  $\text{O}_2$ . Disk potential scanned at 5 mV/s.

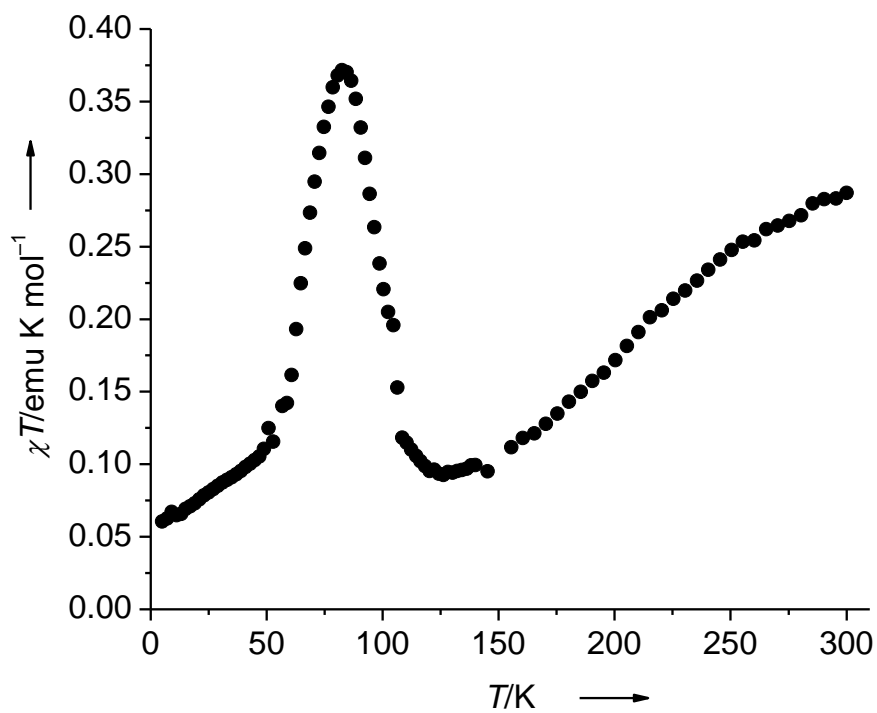


**Figure 4.6.** Temperature dependence of the  $\chi T$  value of the Cu(DAT)/Vulcan composite. Data are shown per mole of Cu and corrected for the significant diamagnetism of the Vulcan substrate.

## References

- (1) Gasteiger, H. A.; Kocha, S. S.; Sompalii, B.; Wagner, F. T., Activity Benchmarks and Requirements for Pt, Pt-Alloy, and Non-Pt Oxygen Reduction Catalysts for PEMFCs. *Appl. Catal., B* **2005**, *56*, 9-35.
- (2) Mano, N.; Soukharev, V.; Heller, A., A Laccase-Wiring Redox Hydrogel for Efficient Catalysis of O<sub>2</sub> Electroreduction. *J. Phys. Chem. B* **2006**, *110*, 11180-11187.
- (3) Blanford, C. F.; Heath, R. S.; Armstrong, F. A., A Stable Electrode for High-Potential, Electrocatalytic O<sub>2</sub> Reduction Based on Rational Attachment of a Blue Copper Oxidase to a Graphite Surface. *Chem. Commun. (Cambridge, U. K.)* **2007**, 1710-1712.
- (4) Zhang, J.; Anson, F. C., Complexes of Cu(II) with Electroactive Chelating Ligands Adsorbed on Graphite Electrodes: Surface Coordination Chemistry and Electrocatalysis. *J. Electroanal. Chem.* **1993**, *348*, 81-97.
- (5) Dias, V. L. N.; Fernandes, E. N.; da Silva, L. M. S.; Marques, E. P.; Zhang, J.; Marques, A. L. B., Electrochemical Reduction of Oxygen and Hydrogen Peroxide Catalyzed by a Surface Copper(II)-2,4,6-Tris(2-Piridil)-1,3,5-Triazine Complex Adsorbed on a Graphite Electrode. *J. Power Sources* **2005**, *142*, 10-17.
- (6) Zhang, J.; Anson, F. C., Electrochemistry of the Cu(II) Complex of 4,7-Diphenyl-1,10-Phenanthrolinedisulfonate Adsorbed on Graphite Electrodes and Its Behavior as an Electrocatalyst for the Reduction of O<sub>2</sub> and H<sub>2</sub>O<sub>2</sub>. *J. Electroanal. Chem.* **1992**, *341*, 323-341.
- (7) McCrory, C. C. L.; Ottenwaelder, X.; Stack, T. D. P.; Chidsey, C. E. D., Kinetic and Mechanistic Studies of the Electrocatalytic Reduction of O<sub>2</sub> to H<sub>2</sub>O with Mononuclear Cu Complexes of Substituted 1,10-Phenanthrolines. *J. Phys. Chem. A* **2007**, *111*, 12641-12650.
- (8) Cai, C. X.; Xue, K. H.; Xu, X. Y.; Luo, Q. H., Electrocatalysis for the Reduction of O<sub>2</sub> and H<sub>2</sub>O<sub>2</sub> Based on Complex of Copper(II) with the Tris(3-Aminopropyl)Amine and Imidazole Ligands. *J. Appl. Electrochem.* **1997**, *27*, 793-798.
- (9) Wang, M.; Xu, X.; Gao, J.; Jia, N.; Cheng, Y., Electrocatalytic Reduction of O<sub>2</sub> at Pyrolytic Graphite Electrode Modified by a Novel Copper(II) Complex with 2-[Bis(2-Aminoethyl)Amino]Ethanol and Imidazole Ligands. *Russ. J. Electrochem.* **2006**, *42*, 878-881.
- (10) Slowinski, K.; Kublik, Z.; Bilewicz, R.; Pietraszkiewicz, M., Electrocatalysis of Oxygen Reduction by a Copper(II) Hexaazamacrocyclic Complex. *Chem. Commun. (Cambridge, U. K.)* **1994**, 1087-1088.

- (11) Weng, Y. C.; Fan, F. R. F.; Bard, A. J., Combinatorial Biomimetics. Optimization of a Composition of Copper(II) Poly-L-Histidine Complex as an Electrocatalyst for O<sub>2</sub> Reduction by Scanning Electrochemical Microscopy. *J. Am. Chem. Soc.* **2005**, *127*, 17576-17577.
- (12) Kim, J.; Gewirth, A. A., Electrocatalysis of Oxygen Reduction by Cu-Containing Polymer Films on Glassy Carbon Electrodes. *Bull. Korean Chem. Soc.* **2007**, *28*, 1322-1328.
- (13) Shin, H.; Lee, D.-H.; Kang, C.; Karlin, K. D., Electrocatalytic Four-Electron Reductions of O<sub>2</sub> to H<sub>2</sub>O with Cytochrome C Oxidase Model Compounds. *Electrochim. Acta* **2003**, *48*, 4077-4082.
- (14) Aznar, E.; Ferrer, S.; Borrás, J.; Lloret, F.; Liu-González, M.; Rodríguez-Prieto, H.; García-Granda, S., Coordinative Versatility of Guanazole [3,5-Diamino-1,2,4-Triazole]: Synthesis, Crystal Structure, Epr, and Magnetic Properties of a Dinuclear and a Linear Trinuclear Copper(II) Complex Containing Small Bridges and Triazole Ligands. *Eur. J. Inorg. Chem.* **2006**, *2006*, 5115-5125.
- (15) Paulus, U. A.; Schmidt, T. J.; Gasteiger, H. A.; Behm, R. J., Oxygen Reduction on a High-Surface Area Pt/Vulcan Carbon Catalyst: A Thin-Film Rotating Ring-Disk Electrode Study. *J. Electroanal. Chem.* **2001**, *495*, 134-145.
- (16) Bard, A. J.; Faulkner, L. R., *Electrochemical Methods: Fundamentals and Applications*. Wiley: New York, 2001.

## CHAPTER 5. Poisoning the Oxygen Reduction Reaction on Carbon-Supported Fe and Cu Electrocatalysts: Evidence for Metal-Centered Activity

*Reproduced with permission from The Journal of Physical Chemistry Letters, 2011, 2, pp 295–298. Copyright © 2011 American Chemical Society.*

The potential utility of fuel cells as efficient devices for electrical power generation has led to long-standing interest in the oxygen reduction reaction (ORR).<sup>1-3</sup> In spite of a large thermodynamic driving force ( $E^\circ = 1.2 \text{ V}_{\text{RHE}}$ ), the ORR is kinetically slow in the absence of electrocatalysts. Currently, electrocatalysts based on platinum and other precious metals are of the greatest technological significance, but the scarcity and high cost of these materials motivates research efforts aimed at developing non-precious metal (NPM) electrocatalysts for the ORR. Two NPM electrocatalysts of current interest are materials prepared from insoluble complexes of copper with 3,5-diamino-1,2,4-triazole supported on carbon (CuDAT) and heat treated materials containing iron coordinated to nitrogen supported on carbon (Fe/N/C).<sup>4-5</sup>

The remarkable activity of the multicopper active site of laccase, which is capable of reducing oxygen with greater efficiency than Pt,<sup>6</sup> inspired the synthesis of CuDAT.<sup>4</sup> Evaluation of CuDAT as a cathode catalyst in alkaline fuel cells found it to have a mass activity greater than Pt or Ag catalysts (albeit with lower absolute performance).<sup>7</sup> For the first time, the presence of synthetic multicopper sites on an electrode was demonstrated in CuDAT supported on carbon black using magnetic susceptibility measurements.<sup>4</sup> However, experimental confirmation that these multicopper sites are the active sites for the ORR has been lacking.



The preparation of heat treated Fe/N/C electrocatalysts originated as it was found that heat treating carbon supported iron porphyrins and iron phthalocyanines leads to increased stability and activity (even though the macrocycle is decomposed), subsequent work showed that simpler Fe and N precursors (such as iron(II) acetate and ammonia) can also be used to form active materials.<sup>8-9</sup> Recent work has shown that the activity of highly optimized Fe/N/C electrocatalysts can rival that of Pt.<sup>5</sup> Although further research is required to enhance the stability of these materials, they are extremely promising NPM electrocatalysts.

The nature of the ORR active sites in the heat treated Fe/N/C catalysts is controversial. The presence of Fe<sup>2+</sup> coordinated to nitrogen sites has been observed by a variety of analytical techniques; it is also known that iron must be present during heat treatment to form the most active materials.<sup>10-12</sup> Almost 30 years ago Yeager proposed a model for the ORR active site in which the heat treated macrocycles are broken down to form surface nitrogen sites that coordinate transition metals remaining from the parent macrocycle, present as impurities in the carbon support, or deliberately added after pyrolysis.<sup>11, 13-14</sup> However, “metal-free” materials containing carbon and nitrogen are known to exhibit ORR activity, particularly in base, and it has been argued that iron is only required as a catalyst to form a highly ORR active site containing nitrogen and carbon that does not utilize an iron center for oxygen reduction.<sup>15-18</sup> Recent results indicating that Fe/N/C electrocatalysts are not poisoned by CO may also indicate that the reactivity is not iron-centered,<sup>19</sup> while other researchers argue that CO is merely a poor choice of poison.<sup>20</sup>

In this work we utilize carbon supported iron(II) phthalocyanine (FePc) and FePc that has been pyrolyzed at 800 °C as well-known examples of Fe/N/C electrocatalysts and examine their ORR activity in the presence of a range compounds known to coordinate to metal centers. Anionic reagents are likely superior to CO as potential ORR inhibitors because they may be present in solution at the same time as oxygen, whereas CO is displaced upon sparging the solution with oxygen. Although FePc and pyrolyzed FePc have lower activity than the best Fe/N/C materials, they were chosen in this study for consistency with prior poisoning studies and their facile preparation. We also evaluate the ORR activity of CuDAT in the presence of various poisons.

The ORR activity of CuDAT in pH 6 phosphate buffer is shown in Figure 5.1 along with the ORR activity in the presence of 10 mM concentrations of sodium fluoride, potassium thiocyanate, ethanethiol, and sodium azide. Thiocyanate and ethanethiol cause a ~200 mV decrease in the onset potential of the ORR, reduced diffusion-limited currents, and irreproducibility between the anodic and cathodic scans of the rotating disk electrode (RDE) measurements in the mass-transport-dominated regions of the voltammograms (at higher current densities), indicative of a significant poisoning effect. In the presence of fluoride, there is a comparable decrease of ~200 mV in the ORR onset potential; however, the anodic and cathodic scans overlay one another and a diffusion limited current is not observed. Azide does not affect the onset potential or diffusion-limited current, although there is a small decrease in current density at intermediate potentials.

The significant decrease of the ORR activity of CuDAT in the presence of fluoride, thiocyanate, and ethanethiol indicates that the Cu-site is the active site for O<sub>2</sub>

binding and reduction as these poisons are known to coordinate to Cu complexes.<sup>21</sup> Rinsing a thiocyanate-poisoned electrode with water leads to almost complete recovery of the ORR activity in fresh electrolyte without thiocyanate. This indicates that the thiocyanate does not permanently bind to or alter the active site, but rather interacts with the active site in competition with O<sub>2</sub>. The lack of a significant change in the ORR activity of CuDAT in the presence of azide is initially surprising as azide is well known to inhibit laccase and form copper complexes. However, the azide affinity of copper complexes is known to follow a largely electrostatic trend.<sup>22</sup> Therefore, the low azide affinity of CuDAT is reasonable because CuDAT is a neutral complex (the charge on the copper(II) centers is balanced by coordinated sulfate anions) and an aqueous electrolyte is present.

The ORR activity of FePc and pyrolyzed FePc in pH 6 phosphate buffer is shown in Figures 5.2 and 5.3 respectively along with the ORR activity in the presence of 10 mM concentrations of sodium fluoride, potassium thiocyanate, and ethanethiol. With fluoride and thiocyanate, there is no significant change in the ORR activity. With ethanethiol, there are small reductions in the current density that are less pronounced after pyrolysis, but the onset potential of the ORR is not significantly affected. The absence of poisoning by fluoride or thiocyanate is similar to the lack of poisoning by carbon monoxide seen previously.<sup>20</sup> The small effect of ethanethiol on the ORR is not conclusive evidence of iron-centered activity. While ethanethiol is expected to coordinate to a metal center, it is neutral at pH 6, and might also adsorb to a nonmetallic site.

After the absence of conclusive poisoning with the above reagents, the ORR activity of FePc before and after pyrolysis was evaluated in the presence of potassium

cyanide because cyanide is known to form very strong complexes with iron and poison the ORR at iron centers.<sup>23-25</sup> Figure 5.4 shows the RDE measurements of the oxygen reduction activity of FePc and pyrolyzed FePc in 0.1 M NaOH with and without the addition of 10 mM KCN. In the presence of cyanide, the onset potential of both materials is decreased significantly by ~200 mV and the diffusion-limited current is decreased slightly. These results are consistent with those originally obtained by Yeager's group on an unpyrolysed FePc derivative showing a poisoning effect with cyanide in base.<sup>25</sup> In this electrolyte, the pyrolyzed FePc has a slightly lower ORR activity than FePc that is not heat treated; however, it is poisoned to a lesser degree and has a higher activity than unpyrolysed FePc in the presence of cyanide.

Rinsing cyanide poisoned FePc and pyrolyzed FePc electrodes with water results in almost complete recovery of the ORR activity in fresh electrolyte without cyanide. This indicates that cyanide competes with O<sub>2</sub> for access to the active site, but does not permanently bind to or alter the active site. Thiocyanate does not affect the ORR activity of FePc or pyrolyzed FePc in 0.1 M NaOH indicating that the inhibition in the above experiments is due to cyanide binding and not an artifact arising from the change in electrolyte pH. Prior studies found that a shift from a four-electron to a two-electron ORR pathway occurs upon cyanide poisoning of iron-based electrocatalysts.<sup>24-25</sup> We employed a relatively high electrocatalyst loading (~0.8 mg cm<sup>-2</sup>) in this study, and it has been demonstrated that this loading level obscures the ORR mechanism of Fe/N/C electrocatalysts.<sup>26</sup> It is therefore not surprising that no shift in mechanism is apparent in this study.

The marked decrease in the ORR onset potential of FePc and pyrolyzed FePc in the presence of cyanide strongly suggests that the active sites in these materials are iron-centered both before and after pyrolysis. The inability of fluoride, thiocyanate, or ethanethiol to poison the ORR could indicate that the site is either remarkably labile or has a high affinity for O<sub>2</sub>. Cyanide is well-known to bind to a wide variety of iron(II) and iron(III) complexes,<sup>23</sup> so it is difficult to speculate about the exact nature of the iron site on the basis of these data. However, it is clear that the absence of poisoning by anions or small molecules other than cyanide is not sufficient to indicate a metal-free active site in these materials. These results are consistent with Yeager's original proposal that upon heat treatment, Fe macrocycles decompose to form a nitrogen-enriched surface that provides coordination sites for iron that make up the active sites for the ORR.<sup>14</sup>

In conclusion, CuDAT is resistant to poisoning by azide, but is poisoned by fluoride and other metal coordinating ligands consistent with an active site containing a neutral copper(II) complex. The Fe/N/C electrocatalysts are remarkably resilient to many metal-binding ligands, but slight poisoning by EtSH and significant poisoning by KCN are consistent with an iron-centered active site, even after pyrolysis. With these assurances, further design of metal-centered complexes for the ORR can proceed.

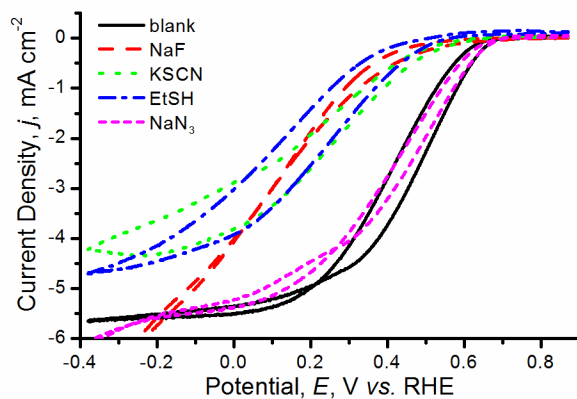


**Figure 5.1.** RDE measurements of the oxygen reduction activity of carbon supported CuDAT in  $\text{O}_2$ -saturated pH 6 phosphate buffer alone (black) and containing 10 mM NaF (red), 10 mM KSCN (green), 10 mM EtSH (blue), or 10 mM  $\text{NaN}_3$  (magenta). Data were recorded at 1600 rpm and  $5 \text{ mV s}^{-1}$ .

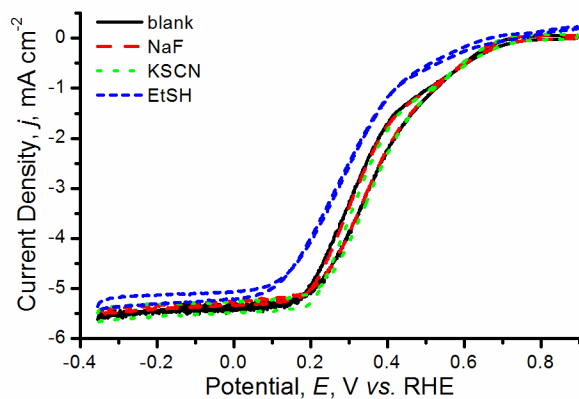


**Figure 5.2.** RDE measurements of the oxygen reduction activity of carbon supported FePc in O<sub>2</sub>-saturated pH 6 phosphate buffer alone (black) and containing 10 mM NaF (red), 10 mM KSCN (green), or 10 mM EtSH (blue). Data were recorded at 1600 rpm and 5 mV s<sup>-1</sup>.

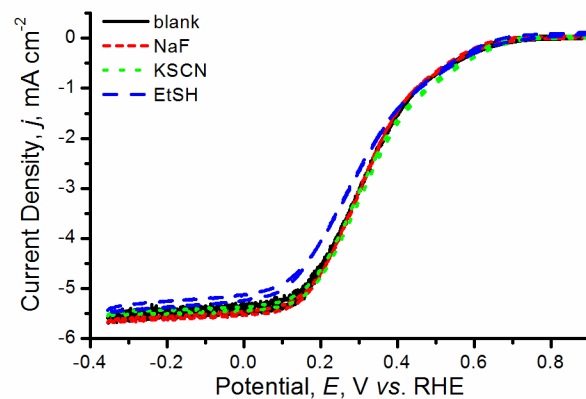


**Figure 5.3.** RDE measurements of the oxygen reduction activity of pyrolyzed carbon supported FePc in  $\text{O}_2$ -saturated pH 6 phosphate buffer alone (black) and containing 10 mM NaF (red), 10 mM KSCN (green), or 10 mM EtSH (blue). Data were recorded at 1600 rpm and  $5 \text{ mV s}^{-1}$ .



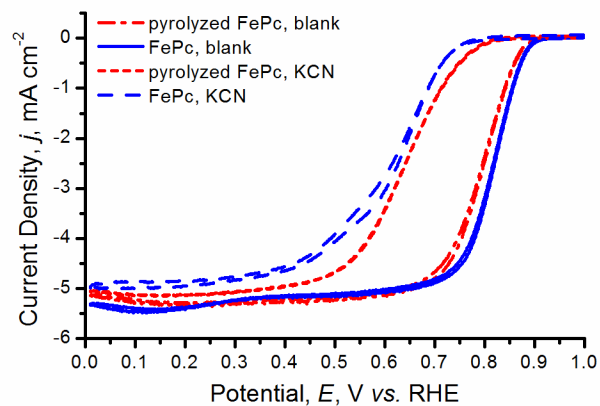


**Figure 5.4.** RDE measurements of the oxygen reduction activity of carbon supported FePc (blue lines) and pyrolyzed carbon supported FePc (red lines) in O<sub>2</sub>-saturated 0.1 M NaOH alone (solid and dash dot lines) and containing 10 mM KCN (long and short dashed lines). Data were recorded at 1600 rpm and 5 mV s<sup>-1</sup>.

## References

- (1) Gewirth, A. A.; Thorum, M. S., Electroreduction of Dioxygen for Fuel-Cell Applications: Materials and Challenges. *Inorg. Chem.* **2010**, *49*, 3557-3566.
- (2) Gasteiger, H. A.; Markovic, N. M., Just a Dream-or Future Reality? *Science* **2009**, *324*, 48-49.
- (3) Wagner, F. T.; Lakshmanan, B.; Mathias, M. F., Electrochemistry and the Future of the Automobile. *J. Phys. Chem. Lett.* **2010**, *1*, 2204-2219.
- (4) Thorum, M. S.; Yadav, J.; Gewirth, A. A., Oxygen Reduction Activity of a Copper Complex of 3,5-Diamino-1,2,4-Triazole Supported on Carbon Black. *Angew. Chem., Int. Ed.* **2009**, *48*, 165-167.
- (5) Lefevre, M.; Proietti, E.; Jaouen, F.; Dodelet, J. P., Iron-Based Catalysts with Improved Oxygen Reduction Activity in Polymer Electrolyte Fuel Cells. *Science* **2009**, *324*, 71-74.
- (6) Thorum, M. S.; Anderson, C. A.; Hatch, J. J.; Campbell, A. S.; Marshall, N. M.; Zimmerman, S. C.; Lu, Y.; Gewirth, A. A., Direct, Electrocatalytic Oxygen Reduction by Laccase on Anthracene-2-Methanethiol-Modified Gold. *J. Phys. Chem. Lett.* **2010**, *1*, 2251-2254.
- (7) Brushett, F. R.; Thorum, M. S.; Lioutas, N. S.; Naughton, M. S.; Tornow, C.; Jhong, H. R.; Gewirth, A. A.; Kenis, P. J. A., A Carbon-Supported Copper Complex of 3,5-Diamino-1,2,4-Triazole as a Cathode Catalyst for Alkaline Fuel Cell Applications. *J. Am. Chem. Soc.* **2010**, *132*, 12185-12187.
- (8) Bezerra, C. W. B.; Zhang, L.; Lee, K. C.; Liu, H. S.; Marques, A. L. B.; Marques, E. P.; Wang, H. J.; Zhang, J. J., A Review of Fe-N/C and Co-N/C Catalysts for the Oxygen Reduction Reaction. *Electrochim. Acta* **2008**, *53*, 4937-4951.
- (9) Zagal, J. H., Metallophthalocyanines as Catalysts in Electrochemical Reactions. *Coord. Chem. Rev.* **1992**, *119*, 89-136.
- (10) Faubert, G.; Côté, R.; Dodelet, J. P.; Lefèvre, M.; Bertrand, P., Oxygen Reduction Catalysts for Polymer Electrolyte Fuel Cells from the Pyrolysis of Fe<sup>II</sup> Acetate Adsorbed on 3,4,9,10-Perylenetetracarboxylic Dianhydride. *Electrochim. Acta* **1999**, *44*, 2589-2603.
- (11) Scherson, D. A.; Yao, S. B.; Yeager, E. B.; Eldridge, J.; Kordesch, M. E.; Hoffman, R. W., In Situ and Ex Situ Moessbauer Spectroscopy Studies of Iron Phthalocyanine Adsorbed on High Surface Area Carbon. *J. Phys. Chem.* **1983**, *87*, 932-943.

- (12) Lefevre, M.; Dodelet, J. P.; Bertrand, P., Molecular Oxygen Reduction in PEM Fuel Cells: Evidence for the Simultaneous Presence of Two Active Sites in Fe-Based Catalysts. *J. Phys. Chem. B* **2002**, *106*, 8705-8713.
- (13) Gupta, S.; Tryk, D.; Bae, I.; Aldred, W.; Yeager, E., Heat-Treated Polyacrylonitrile-Based Catalysts for Oxygen Electroreduction. *J. Appl. Electrochem.* **1989**, *19*, 19-27.
- (14) Yeager, E., Electrocatalysts for O<sub>2</sub> Reduction. *Electrochim. Acta* **1984**, *29*, 1527-1537.
- (15) Maldonado, S.; Stevenson, K. J., Direct Preparation of Carbon Nanofiber Electrodes Via Pyrolysis of Iron(II) Phthalocyanine: Electrocatalytic Aspects for Oxygen Reduction. *J. Phys. Chem. B* **2004**, *108*, 11375-11383.
- (16) Biddinger, E.; von Deak, D.; Ozkan, U., Nitrogen-Containing Carbon Nanostructures as Oxygen-Reduction Catalysts. *Top. Catal.* **2009**, *52*, 1566-1574.
- (17) Gong, K.; Du, F.; Xia, Z.; Durstock, M.; Dai, L., Nitrogen-Doped Carbon Nanotube Arrays with High Electrocatalytic Activity for Oxygen Reduction. *Science* **2009**, *323*, 760-764.
- (18) Yu, D.; Nagelli, E.; Du, F.; Dai, L., Metal-Free Carbon Nanomaterials Become More Active Than Metal Catalysts and Last Longer. *J. Phys. Chem. Lett.* **2010**, *1*, 2165-2173.
- (19) Maldonado, S.; Stevenson, K. J., Influence of Nitrogen Doping on Oxygen Reduction Electrocatalysis at Carbon Nanofiber Electrodes. *J. Phys. Chem. B* **2005**, *109*, 4707-4716.
- (20) Birry, L.; Zagal, J. H.; Dodelet, J.-P., Does CO Poison Fe-Based Catalysts for ORR? *Electrochem. Commun.* **2010**, *12*, 628-631.
- (21) Conry, R. R., Copper: Inorganic & Coordination Chemistry. In *Encyclopedia of Inorganic Chemistry*, John Wiley & Sons, Ltd: 2006.
- (22) Casella, L.; Gullotti, M.; Pallanza, G.; Buga, M., Spectroscopic and Binding Studies of Azide-Copper(II) Model Complexes. *Inorg. Chem.* **1991**, *30*, 221-227.
- (23) Burgess, J.; Twigg, M. V., Iron: Inorganic & Coordination Chemistry. In *Encyclopedia of Inorganic Chemistry*, John Wiley & Sons, Ltd: 2006.
- (24) Li, W.; Yu, A.; Higgins, D. C.; Llanos, B. G.; Chen, Z., Biologically Inspired Highly Durable Iron Phthalocyanine Catalysts for Oxygen Reduction Reaction in Polymer Electrolyte Membrane Fuel Cells. *J. Am. Chem. Soc.* **2010**, *132*, 17056-17058.

- (25) Gupta, S.; Fierro, C.; Yeager, E., The Effects of Cyanide on the Electrochemical Properties of Transition-Metal Macrocycles for Oxygen Reduction in Alkaline-Solutions. *J. Electroanal. Chem.* **1991**, *306*, 239-250.
- (26) Bonakdarpour, A.; Lefevre, M.; Yang, R. Z.; Jaouen, F.; Dahn, T.; Dodelet, J. P.; Dahn, J. R., Impact of Loading in RRDE Experiments on Fe-N-C Catalysts: Two- or Four-Electron Oxygen Reduction? *Electrochem. Solid-State Lett.* **2008**, *11*, B105-B108.

## Appendix A. Gold Roughening Macro

Macro commands for roughing Au electrodes on a CH Instruments potentiostat:

```
tech: ssf
sens: 1e-2
qt=0
ei1=-0.25
ef1=1.25
v1=1
es1=1.25
st1=1.3
ei2=1.25
ef2=-0.25
v2=0.5
es2=-0.25
st2=10
for: 25
run
next
```

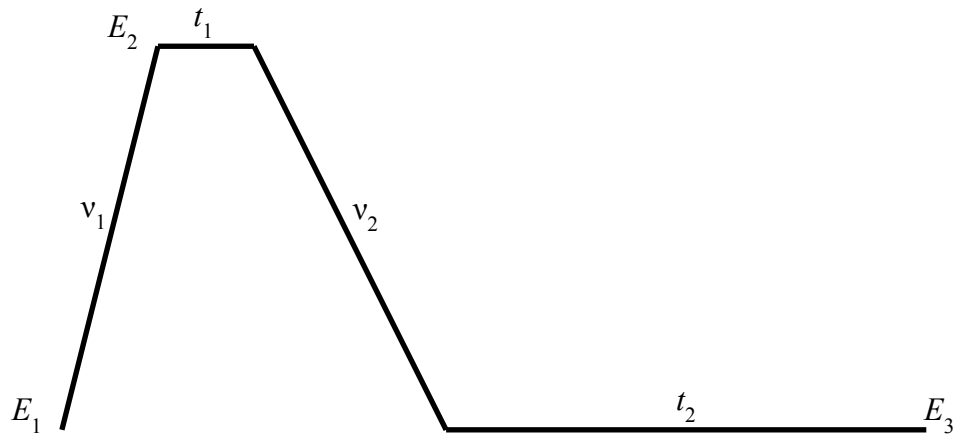


**Figure A.1.** Schematic of the potential waveform generated by the macro.

$E_1 = E_3 = -0.25$  V (Ag/AgCl),  $E_2 = 1.25$  V (Ag/AgCl),

$v_1 = 1$  V/s,  $v_2 = 0.5$  V/s,  $t_1 = 1.3$  s,  $t_2 = 10$  s,

$N = 25$  cycles.

## Author's Curriculum Vitae

### Education

---

- PhD, Chemistry**, University of Illinois at Urbana-Champaign, Urbana IL May 2011  
Dissertation title: "Oxygen Reduction Electrocatalysis" GPA 3.80/4.00  
Adviser: Professor Andrew A. Gewirth
- BS with Honors**, Chemistry, University of Utah, Salt Lake City UT 2005  
Thesis title: "Synthesis of Molecule-based Magnetic Materials" GPA 3.69/4.00  
Adviser: Professor Joel S. Miller

### Research Experience

---

- Graduate Research Assistant**, University of Illinois with Prof. Andrew Gewirth 2005-2011
- Discovered a new class of oxygen reduction catalysts for fuel cells based on copper triazole complexes
  - Characterized electrocatalysts using electrochemistry (including rotating ring-disk electrode voltammetry), spectroscopy (FT-IR, UV-Vis, XPS, Raman), elemental microanalysis, and XRD
  - Supervised and directed the work of 4 undergraduate students
- Undergraduate Research Assistant**, University of Utah with Prof. Joel Miller 2003-2005
- Synthesized air-sensitive inorganic compounds using Schlenk-line and glove box techniques
  - Characterized the magnetic properties of molecule-based materials using Quantum Designs MPMS and PPMS systems, FT-IR, and UV-Vis spectroscopies
- Intern**, Watson Pharmaceuticals, Salt Lake City UT, Transdermal Research Department 2002
- Developed analytical methods utilizing ATR-FTIR, HPLC, and GC to assay the drug concentrations in the individual layers of skin patches for transdermal drug delivery

### Publications

---

**Thorum, M. S.;** Hankett, J. M.; Gewirth A. A., Poisoning the Oxygen Reduction Reaction on Carbon Supported Fe and Cu Electrocatalysts: Evidence for Metal-Centered Activity. *Journal of Physical Chemistry Letters* **2011**, 2, 295-298.

Brushett, F. R.; **Thorum, M. S.;** Lioutas, N. S.; Naughton, M. S.; Tornow, C.; Jhong, H.; Gewirth, A. A.; Kenis, P. J., A Carbon-Supported Copper Complex of 3,5-Diamino-1,2,4-triazole as a Cathode Catalyst for Alkaline Fuel Cell Applications. *Journal of the American Chemical Society* **2010**, 132, 12185-12187.

**Thorum, M. S.;** Anderson, C. A.; Hatch, J. J.; Campbell, A. S.; Marshall, N. M.; Zimmerman, S. C.; Lu, Y.; Gewirth, A. A., Direct, Electrocatalytic Oxygen Reduction by Laccase on Anthracene-2-methanethiol-Modified Gold. *Journal of Physical Chemistry Letters* **2010**, *1*, 2251-2254.

Gewirth, A. A.; **Thorum, M. S.**, Electroreduction of Dioxygen for Fuel-Cell Applications: Materials and Challenges. *Inorganic Chemistry* **2010**, *49*, 3557-3566.

**Thorum, M. S.;** Yadav, J.; Gewirth, A. A., Oxygen Reduction Activity of a Copper Complex of 3,5-Diamino-1,2,4-triazole Supported on Carbon Black. *Angewandte Chemie-International Edition* **2009**, *48*, (1), 165-167.

**Thorum, M. S.;** Taliaferro, M. L.; Min, K. S.; Miller, J. S., The quest for magnets composed of vanadium and 1,4-benzoquinones. *Polyhedron* **2007**, *26*, (9-11), 2247-2251.

**Thorum, M. S.;** Pokhodnya, K. I.; Miller, J. S., Solvent enhancement of the magnetic ordering temperature ( $T_c$ ) of the room temperature  $V[TCNE]_x$  S (S = solvent, TCNE = tetracyanoethylene;  $x \approx 2$ ) magnet. *Polyhedron* **2006**, *25*, (9), 1927-1930.

Taliaferro, M. L.; **Thorum, M. S.;** Miller, J. S., Room-temperature organic-based magnet ( $T_c \approx 50$  °C) containing tetracyanobenzene and hexacarbonylvandate(-I). *Angewandte Chemie-International Edition* **2006**, *45*, (32), 5326-5331.

Vickers, E. B.; Selby, T. D.; **Thorum, M. S.;** Taliaferro, M. L.; Miller, J. S., Vanadium 7,7,8,8-tetracyano-p-quinodimethane ( $V[TCNQ]_2$ )-based magnets. *Inorganic Chemistry* **2004**, *43*, (20), 6414-6420.

## Teaching Experience

---

**Adventure Recreation Instructor**, University of Illinois 2008-2009

- Assisted in the formation of a rock climbing campus recreation program
- Developed curricula for and taught staff training and climbing clinics

**Graduate Student Instructor**, CHEM 102D General Chemistry I, University of Illinois 2006

- Delivered daily lectures to 2 classes of ~30 students
- Wrote quizzes, graded homework and exams
- Included on the "List of Teachers Ranked as Excellent by their Students"

**Teaching Assistant**, CHEM 104 General Chemistry II, University of Illinois 2005-2006

- Led bi-weekly discussions with 20-25 students
- Graded homework, quizzes, and exams
- Included on the "List of Teachers Ranked as Excellent by their Students"

**Teaching Assistant**, CHEM 2315 Organic Chemistry I Laboratory, University of Utah 2003

- Supervised weekly lab experiments, graded lab reports and exams

## **Leadership Experience**

---

<b>Vice-President</b> , UIUC Climbing Club, University of Illinois	2009-2010
<b>Student Representative</b> , University of Utah College of Science Academic Appeals and Academic Misconduct Committee	2004-2005

## **Awards and Honors**

---

Pytosh Fellowship	2008-2009
Dr. Harold R. Snyder Fellowship	2007-2008
Walter Brown Fellowship	2006-2007
Glen E. and Barbara R. Ullyot Fellowship	2005-2006
University of Utah College of Science Research Scholar Award	2005
Golden Key International Honor Society, member	2005
Walter D. and Grace G. Bonner Memorial Award	2005
Hypercube Scholar Award	2005
ACS Division of Inorganic Chemistry Student Travel Grant	2005
Chemistry Departmental Tuition Waiver Scholarship	2004
Senior Comprehensive Chemistry Exam Prize, for highest score (taken as a Junior)	2004
Crocker Science House Scholar-in-Residence	2003-2005
Watson Pharmaceuticals C <sup>2</sup> C Scholarship	2003
National Merit Scholarship	1999
Honor Society of Phi Kappa Phi, member	1999
Eagle Scout Award	1998
Henry Eyring Analytical Chemistry Scholar	1998

## **Professional Affiliations**

---

American Chemical Society